12

Electrical and Magnetic Properties

Charge movement, electric fields, and voltages play essential roles in the body. The driving forces that induce such charge motion are complicated chemical and biological processes that are only partially understood. The interplay of the resulting charges and fields is physical in nature and is well understood.

We have addressed the importance of electricity in the body only briefly in previous chapters. In Chap. 3 we examined the electromyograms (EMGs) of muscle activity (Fig. 3.12), in Chap. 5 we saw that muscles are activated by electrical stimuli and the release of Ca^{2+} ions, and in Chap. 8 we learned that the polarization and depolarization of cell membranes in the heart provide the signals for electrocardiograms (EKGs, ECGs). We now discuss such electrical interactions in more depth as we focus on the electrical properties of the body, the propagation of electrical signals in the axons of nerves, and electrical potentials in the body (Table 12.1).

It is impossible to overemphasize the importance of this human "bioelectricity." The function of every cell depends on it. Every neuron in the brain, every neuron transmitting any information within the body, every neuron enabling skeletal, cardiac, and smooth muscles is yet another vital example. This chapter is largely a discussion of the physics of the motion of positive and negative ions in the blood and cells. We will be concerned with the motion of these ions across membrane boundaries, as in neurons, but not the underlying biology that controls these ion channels. Electric voltages measured at different places in the body describe electrical activity, as is seen in Table 12.1. We will emphasize the propagation of electrical signals in nerves and monitoring the EKG signals from the heart.

Electric and magnetic fields are closely coupled in many areas of physics; for example, electromagnetic waves (visible light, radio waves, X-rays, and so on) consist of electric and magnetic fields oscillating in phase. Magnetic fields appear when current flows. Although current flow is important in the body, the resulting magnetic fields appear to be relatively unimportant and we will address magnetism in the body only briefly in this chapter. For more details on the electrical and magnetic properties of the body see [566, 579, 581, 586, 594].

Table 12.1. Typical amplitude of bioelectric signals. (Using data from [567, 580])

bioelectric signal	typical amplitude
electrocardiogram (EKG/ECG, heart)	1 mV
electroencephalogram (EEG, brain waves)	10–100 μV
electromyogram (EMG, muscle)	300 μV
transmembrane potential	100 mV
electro-oculogram (EOG, eye)	500 μV

12.1 Review of Electrical Properties

We first review the various elements of electrostatics and current flow needed to understand electricity in the body, including the flow of an electrical pulse along an axon.

The electric field at a distance r caused by a point charge q is given by Coulomb's Law:

$$\mathbf{E} = \frac{kq\mathbf{r}}{r^3} = \frac{kq\mathsf{r}}{r^2}, \tag{12.1}$$

where the vector from the charge to the point is $\mathbf{r} = r\mathsf{r}$ and r is a unit vector from that charge to the point of interest, as illustrated in Fig. 12.1a,b. The constant $k = 8.99 \times 10^9\,\text{N-m}^2/\text{C}^2$ for a charge in vacuum, where C stands for coulombs, and can also be expressed as $1/4\pi\epsilon_0$. In a medium of dielectric constant ϵ (where $\epsilon = 1$ in vacuum), $k = 1/4\pi\epsilon_0\epsilon$.

The potential of that charge is

$$V = \frac{kq}{r}. \tag{12.2}$$

and, as here, the potential is usually defined to be zero as r approaches infinity. The potential difference (or voltage) between two points "b" and "a" caused by a field is

$$\Delta V = V_\text{b} - V_\text{a} = -\int_{\mathbf{r}_a}^{\mathbf{r}_b} \mathbf{E} \cdot \text{d}\mathbf{r}. \tag{12.3}$$

This can also be expressed as

$$\mathbf{E} = -\nabla V \tag{12.4}$$

or in one-dimension as

$$E = -\frac{\text{d}V}{\text{d}x}. \tag{12.5}$$

If there are two charges q and $-q$ in vacuum separated, say a distance $\mathbf{d}$ in the d unit vector direction (so the vector between them is $\mathbf{d}$), the electric field

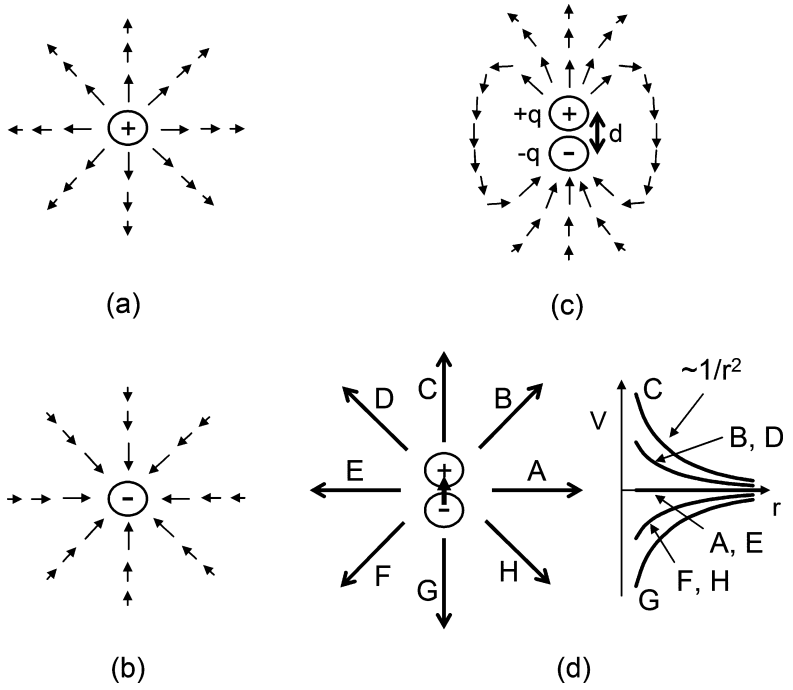

Fig. 12.1. The electric field vectors for (**a**) positive and (**b**) negative charges are shown, along with those for (**c**) a dipole of two charges $+q$ and $-q$, separated by a distance d, so the magnitude of the dipole moment is $P = qd$. The direction of the dipole moment is seen by the arrow within the dipole in (**d**). (d) also shows the potential along the different radial directions shown for this dipole, and the $1/r^2$ decrease in each of these voltages

is the vector sum of the contributions from (12.1) and the electric potential is still obtained using (12.3) (Fig. 12.1c,d). For $r \gg d$, the expression for the potential can be simplified to give

$$V = \frac{k\mathbf{P}.\mathbf{r}}{r^3}, \tag{12.6}$$

where $\mathbf{P} = q\mathsf{d}$ is the electric dipole moment vector, which has magnitude $P = qd$ and points in the d direction. If the angle between the dipole vector $\mathbf{P}$ and distance vector $\mathbf{r}$ is θ, then this equation becomes

$$V = \frac{kP\cos\theta}{r^2}. \tag{12.7}$$

Similarly, we can calculate the dipole moment for many charges separated by various distances. Evaluation of the fields caused by such electric dipoles is of particular value when there is no net charge in the collection of charges, as is true most everywhere in the body.

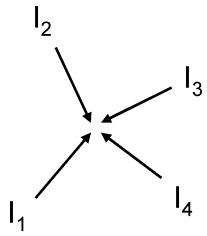

Fig. 12.2. Kirchhoff's 1st Law, showing that the algebraic sum of the current flows to a point must be zero (if charge is not accumulating or being depleted at that point). (Note that least one of the current flows must be negative, i.e., it must point outward)

Now let us consider a moving particle with charge q (in coulombs, C), the current, $I = \mathrm{d}q/\mathrm{d}t$, associated with such a charge or charges (which is the change in charge per unit time), and the associated current density, $J = I/A$ (which is the current flowing per unit area A). Charge is conserved, meaning that it is neither created nor lost. It also means that the vector sum of all currents entering a volume or a small volume element (such as a node) is zero in steady state (Fig. 12.2). This conservation of current (and charge) is known as Kirchhoff's 1st Law

$$\sum_n I_n = 0. \tag{12.8}$$

(The direction of current flow is important here, even thought the current is being expressed as a scalar.)

When a current flows along a material with *resistance* R (in ohms, Ω) (which we called R_{elect} in other chapters), there is a voltage drop V (in volts V) (which we called V_{elect} in other chapters) across the material given by Ohm's Law (Fig. 12.3a)

$$V = IR. \tag{12.9}$$

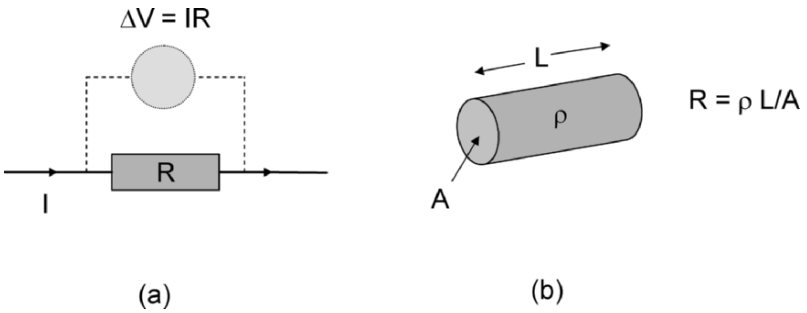

Fig. 12.3. (**a**) Ohm's Law and (**b**) evaluating resistance R from resistivity ρ

The resistance is an extensive property that depends on the intensive property *resistivity* ρ of the material, and the cross-sectional area A and length L of the structure (Fig. 12.3b)

$$R = \frac{\rho L}{A}. \tag{12.10}$$

For a cylinder with radius a, we have $A = \pi a^2$ and $R = \rho L/\pi a^2$. More generally, for a structure with uniform cross-section, the resistance R is proportional to length and we can define a resistance per unit length

$$r = \frac{R}{L} = \frac{\rho}{A}, \tag{12.11}$$

which equals $\rho/\pi a^2$ for conduction along a cylinder. The conductance G (units S (siemens), $1\,\mathrm{S} = 1\,\mathrm{mho} = 1/\mathrm{ohm} = 1/\Omega$) is $1/R$, the conductivity is $\sigma = 1/\rho$, and the conductance per unit area $g = G/A = 1/RA = 1/\rho L$. In the body, charged ions, such as Na^+, K^+, Ca^{2+}, Cl^-, and negatively-charged proteins, are the important carriers of charge. Electrons are the charge carriers in most man-made electronic circuits.

A voltage or potential difference V can also develop between two structures, one with a charge $+q$ and the other with charge $-q$, because of the electric fields that run from one to the other. This voltage is

$$V = \frac{q}{C}, \tag{12.12}$$

where C is the capacitance (in farads, F) of the system (called C_{elect} in other chapters). The capacitance C depends on the geometry of these two structures. For example, they could be two parallel plates or two concentric cylinders (Fig. 12.4), which is similar to the axon of a neuron.

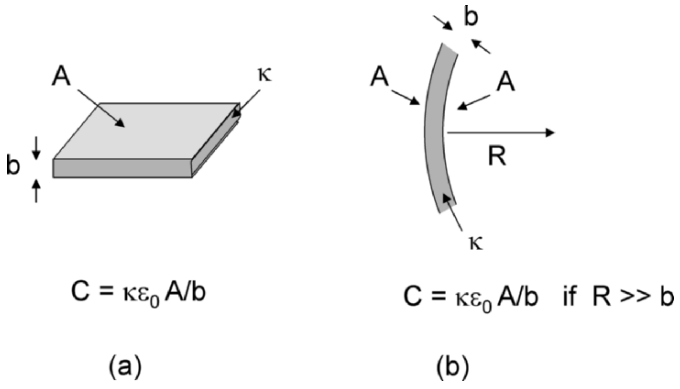

Fig. 12.4. Capacitance for (**a**) parallel plates and (**b**) cylindrical shells

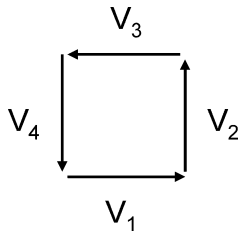

Fig. 12.5. Kirchhoff's 2nd Law, showing that the algebraic sum of the potential drops (voltages) along a closed loop is zero

For two parallel plates with area A separated a distance b by an insulator with dielectric constant κ, we see

$$C_{\text{parallel plates}} = \frac{\kappa\epsilon_0 A}{b}. \tag{12.13}$$

The charge density on each plate is $\sigma = q/A$.

The algebraic sum of all voltages along a closed loop circuit equals zero (Fig. 12.5). This is known as Kirchhoff's 2nd Law

$$\sum_n V_n = 0. \tag{12.14}$$

12.2 Electrical Properties of Body Tissues

12.2.1 Electrical Conduction through Blood and Tissues

When voltage is applied across a metal, a current flows because electrons move under the influence of an electric field. When a voltage is applied across a solution containing positive and negative ions, current flows because both ions move under the influence of the electric field. The conductivity σ of a solution is the sum of the contributions to the current flow for each ion. For low concentrations of these ions, this contribution is proportional to the concentration n_i for that ion, with a proportionality constant $\Lambda_{0,i}$, so

$$\sigma = \sum_i n_i \Lambda_{0,i}. \tag{12.15}$$

Table 12.2 gives $\Lambda_{0,i}$, the molar conductance at infinite dilution for several common ions, while Table 12.3 gives typical concentrations of common ions in the blood and in cells. The resistance of a path can be determined using $\rho = 1/\sigma$ and $R = \rho L/A$ (12.10).

As with many materials, body tissues have dielectric properties, but still have some conductivity, and therefore can be considered as leaky dielectrics. The resistivity of body tissues is shown in Table 12.4 and Fig. 12.6.

Table 12.2. The molar conductance at infinite dilution $\Lambda_{0,i}$ for different ions. (Using data from [596])

ion	$\Lambda_{0,i}$ (1/ohm-m-M)
H^+	34.9
OH^-	19.8
Na^+	5.0
Cl^-	7.6

Table 12.3. Ionic concentrations in blood and cell cytoplasm of unbound ions. (Using data from [597])

ion	blood concentration	cytoplasm concentration	ratio
Na^+	145 mM	12 mM	12:1
K^+	4 mM	140 mM	1:35
H^+	40 nM	100 nM	1:2.5
Mg^{2+}	1.5 mM	0.8 mM	1.9:1
Ca^{2+}	1.8 mM	100 nM	18:1
Cl^-	115 mM	4 mM	29:1
HCO_3^-	25 mM	10 mM	2.5:1

Table 12.4. Low frequency resistivity of some body tissues, in ohm-m (Ω-m). (Using data from [567, 573, 586])

tissue	resistivity
cerebrospinal fluid	0.650
blood plasma	0.7
whole blood	1.6 (Hct = 45%)
skeletal muscle	
– longitudinal	1.25–3.45
– transverse	6.75–18.0
liver	7
lung	
– inspired	17.0
– expired	8.0
neural tissue (as in brain)	
– gray matter	2.8
– white matter	6.8
fat	20
bone	>40
skin	
– wet	10^5
– dry	10^7

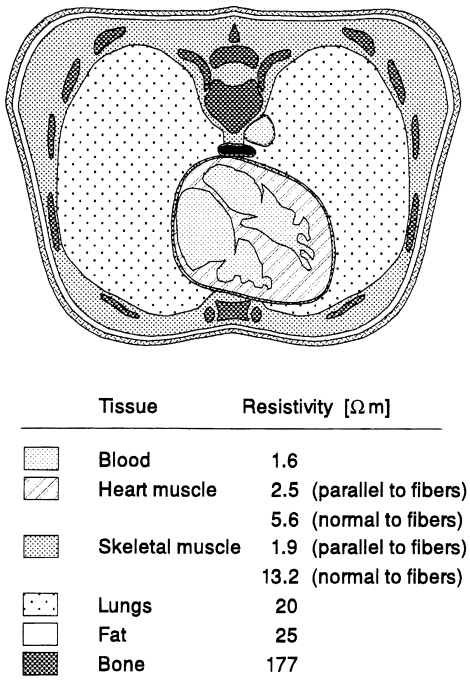

Fig. 12.6. Cross-section of the thorax, with the electrical resistivity of six types of tissues. (From [586]. Used with permission)

12.3 Nerve Conduction

Figure 12.7 shows the structure of nerve cells or neurons with a nucleus, dendrites that receive information across synapses, an axon, and the axon terminals and synapses for signal transmission to other neurons. There are

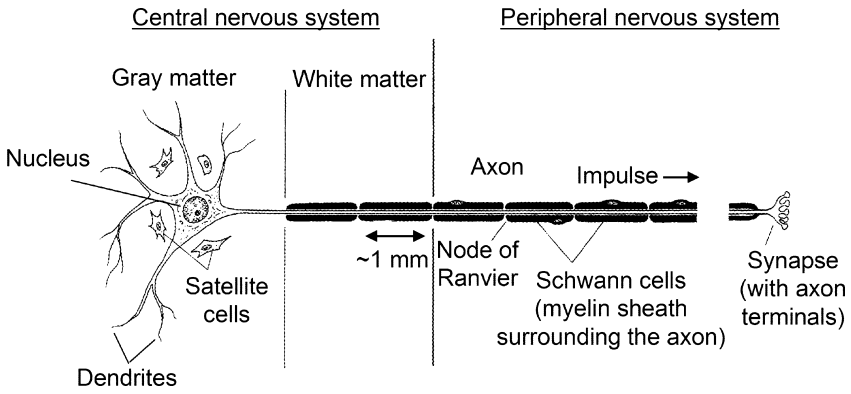

Fig. 12.7. Structure of a neuron. (From [592])

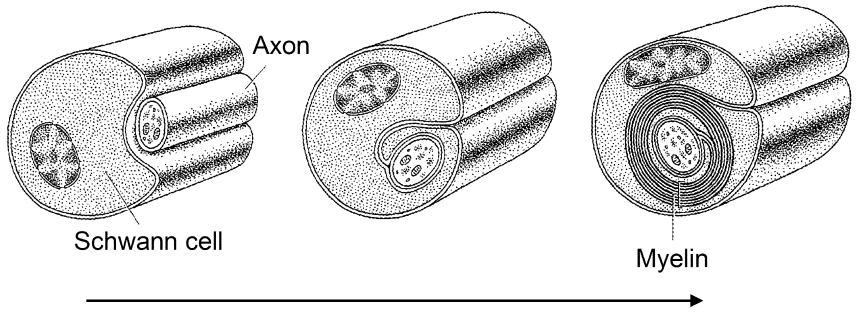

Fig. 12.8. The successive wrapping of Schwann cells about the axon of a neuron to form the myelin sheath of a myelinated nerve. (From [592])

many such neuron axons in a nerve. Unmyelinated axons have no sheath surrounding them. Myelinated axons have myelin sheaths in some regions, which are separated by nodes of Ranvier (ron-vee-ay'). These sheaths are formed by Schwann cells that are wrapped around the axon (Fig. 12.8), with successive wrapped cells separated at a node of Ranvier (Fig. 12.7). We will concentrate on how an electrical impulse travels along such axons.

Approximately 2/3 of the axon fibers in the body are unmyelinated. They have radii of 0.05–0.6 μm and a conduction speed of u (in m/s) $\approx 1.8\sqrt{a}$, where a is the radius of the axon (in μm). Myelinated fibers have outer radii of 0.5–10 μm and a conduction speed of u (in m/s) $\approx 12(a+b) \approx 17a$, where b is the myelin sheath thickness (in μm) (and $a+b$ is the total axon radius). The spacing between the nodes of Ranvier is $\approx 280a$.

Neurons whose axons travel from sensing areas to the spinal cord are called *afferent* neurons or input or sensory neurons. (They are "affected" by conditions that are sensed.) Neurons whose axons leave the ventral surface of the brain stem and the spinal cord to convey signals away from the central nervous system are *efferent neurons* or motor neurons, and these neurons exercise motor control. (They "effect" a change.) There are approximately 10 million afferent neurons, 100 billion neurons in the brain with 100 trillion synapses, and a half a million efferent neurons, so there are roughly 20 sensory neurons for every motor neuron and several thousand central processing neurons for every input or output neuron for processing. Bundles of these neuron axons are called nerves outside of the brain and tracts inside the brain. Details about the nervous system are given in [588].

There are approximately $1 - 2 \times 10^6$ optical nerves from the $1 - 2 \times 10^8$ rods and cones in our eyes, 20,000 nerves from the 30,000 hair cells in our ears, 2,000 nerves from the 10^7 smell cells in our noses, 2,000 nerves from the 10^8 taste sensing cells in our tongues, 10,000 nerves from the 500,000 touch-sensitive cells throughout our body, and many (but an uncertain number of) nerves from the 3×10^6 pain cells throughout our body.

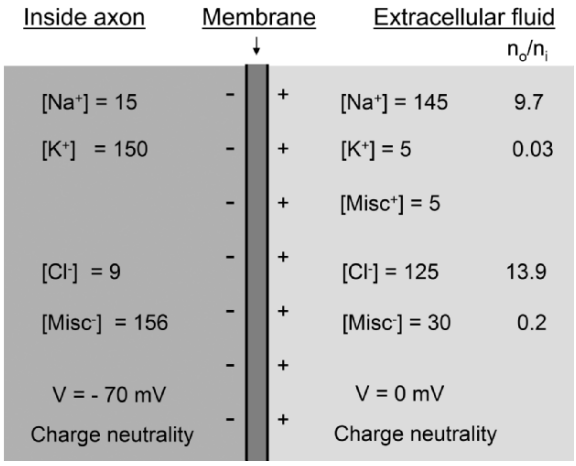

Fig. 12.9. Ion concentrations (in mmol/L) in a typical mammalian axon nerve cell (n_i) and in the extracellular fluid surrounding it (n_o), and their ratios ($n_\mathrm{i}/n_\mathrm{o}$). (Based on [581])

12.3.1 Cell Membranes and Ion Distributions

The cell membrane divides the intracellular and extracellular regions, in neurons and other cells. There are Na^+, K^+, Cl^-, negatively-charged proteins, and other charged species both in the neurons (intracellular) and in the extracellular medium. The concentrations of these ions are such that there is charge neutrality (i.e., an equal number of positive and negative charges) in both the intracellular and extracellular fluids. However, there are negative charges on the inside of the cell membrane and positive charges on the outside of this membrane that produce a *resting potential* of $-70\,\mathrm{mV}$ (Fig. 12.9). This means that the intracellular medium is at $-70\,\mathrm{mV}$, when the *extracellular potential* is arbitrarily defined to be $0\,\mathrm{V}$, as is the custom. Only potential differences are significant, so we are not limiting the analysis by fixing the extracellular potential. This resting potential is the usual potential difference when there is no unusual neural activity. This is known as the *polarized state*. (The propagation of an electrical signal would constitute this type of unusual activity.)

While there is charge neutrality both inside and outside the membrane, the concentrations of each ion are not equal inside and outside the cell, as we will see. The differences in ion concentrations inside and outside the cell membrane are due to a dynamic balance. When there are changes in the permeability of the cell membrane to different charged species, there are transient net charge imbalances that change the potential across the cell membrane. An increase in the membrane potential from $-70\,\mathrm{mV}$, such as to the $-60\,\mathrm{mV}$ seen in Fig. 12.10, is known as *depolarization*, while a decrease from $-70\,\mathrm{mV}$ to say $-80\,\mathrm{mV}$ is called *hyperpolarization*. Depolarization is due to the net flow of

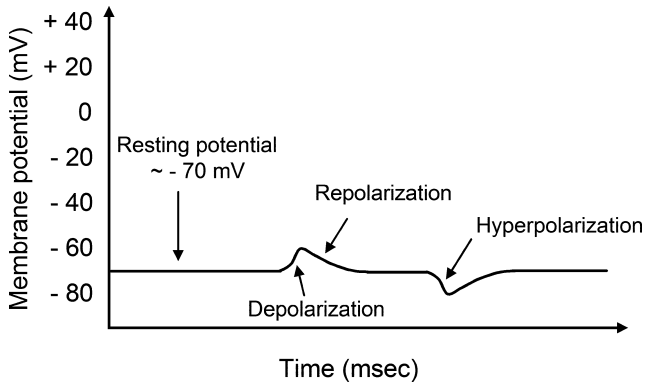

Fig. 12.10. The membrane resting potential of −70 mV (inside the membrane relative to the always fixed 0 mV outside) – the polarized state, along with potential disturbances showing depolarization (voltage increases from the resting potential value), repolarization (returns to the resting potential), and hyperpolarization (decreases from the resting potential)

positive charges into the cell or negative charges to regions outside the cell. Hyperpolarization is due to the net flow of negative charges into the cell or positive charges to outside the cell. Such changes in ion permeability are often termed as changes in the *ion channel*.

Figure 12.9 also shows the concentrations of some of the important charged species inside and outside the cell under resting (i.e., polarized) conditions. We see that there are many more Na^+ outside (145 mmol/L) than inside (15 mmol/L) the cell, but many more K^+ inside (150 mmol/L) than outside (5 mmol/L). Including miscellaneous positive ions outside the cell, there are 165 mmol/L of positive ions both inside and outside the cell. Similarly, there are many more Cl^- outside (125 mmol/L) than inside (9 mmol/L) the cell, but many more miscellaneous negative ions (including proteins) inside (156 mmol/L) than outside (30 mmol/L). There are also 165 mmol/L of negative ions both inside and outside the cell.

There are several driving forces that determine the ionic concentrations, in general, and these intracellular and extracellular concentrations, in particular:

1. There is the natural tendency for concentrations to be uniform everywhere, so when there are concentration gradients across the cell membrane there are flows of these species from the regions of higher concentration to regions of lower concentrations, to equalize the intracellular and extracellular concentrations. This is described by Fick's First Law of Diffusion (7.51), $J_{\text{diff}} = -D_{\text{diff}}\, \mathrm{d}n/\mathrm{d}x$, where J_{diff} is the flux of ions in the x direction (the number of ions flowing across a unit area in a unit time), D_{diff} is the diffusion constant, n is the local concentration of ions, and $\mathrm{d}n/\mathrm{d}x$ is the local concentration gradient.

2. Because the potential is negative inside the cell, we would expect positive ions to enter the cell and be more dominant in the intracellular fluid than the extracellular fluid and for there to be such concentration gradients; this is true for K^+ but not for Na^+. Similarly, we expect negative ions to leave the cell because of the resting potential and be more dominant outside the cell than inside – and again for there to be concentration gradients; this is true for Cl^- but not for the negatively-charged proteins, which form the bulk of the miscellaneous negative ions.
   When charged species are in an electric field, they get accelerated and eventually attain a steady-state drift velocity, v_{drift}, because of collisions that act as a drag force. As shown in Problem 12.7, the drift velocity of a given ion is

$$v_{\text{drift}} = \mu E, \tag{12.16}$$

   where μ is called the mobility and E is the electric field. The flux of ions due to this electric field is

$$J_{\text{elect}} = n v_{\text{drift}} = n \mu E. \tag{12.17}$$

3. The cell membrane permeability and active processes cause the ion concentrations on either side of the membrane to deviate from the values expected from diffusion and the motion of charges in electric fields. The cell membranes are permeable to K^+ and Cl^-, which explains why they behave as expected. Proteins are never permeable to the cell membrane, which is why the concentration of negative-protein ions is unexpectedly high inside. The chemical mechanism called the Na^+ pump (or the Na^+-K^+ pump) actively transports $3Na^+$ from inside to outside the cell for every $2K^+$ it transports from outside to inside the cell; this keeps Na^+ outside the cell and K^+ inside.

The high Na^+ concentration outside the cell is the result of the Na^+ pump fighting against the driving electrical forces and the tendency to equalize concentrations (Fig. 12.11). The high K^+ concentration inside the cell is the result of the electric forces and the Na^+ pump fighting against the tendency to equalize concentrations. The high Cl^- concentration outside the cell is the result of the electrical forces fighting against the tendency to equalize concentrations. The concentration of negative protein ions is unexpectedly high inside because they are large and not permeable to the cell membrane.

Figure 12.12 depicts the directions of motion for charged and neutral molecules for either the random thermal motion in diffusion or the directed effect of an electric field. Figure 12.13 shows how a concentrated band of charged and neutral molecules changes due to either diffusion or an electric field.

Ionic Distributions (Advanced Topic)

What are the expected ionic distributions due to the membrane potential? First, let us consider the expected distributions for several steady state

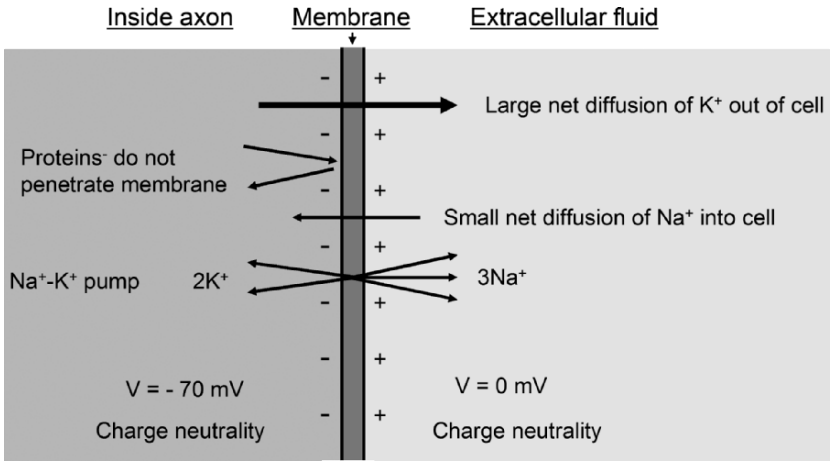

Fig. 12.11. Mechanisms for ion flow across a polarized cell membrane that determine the resting membrane potential

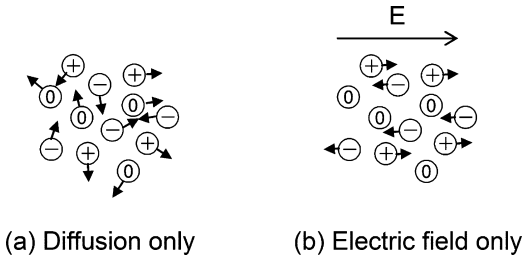

Fig. 12.12. The direction of motion for charged and neutral molecules due to (**a**) diffusion (at a given instant) and (**b**) an electric field

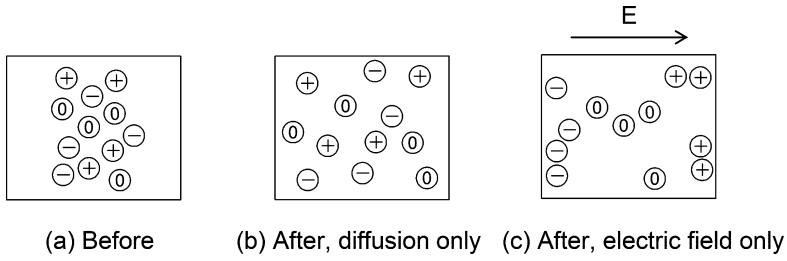

Fig. 12.13. An initial band of charged and neutral molecules (in (**a**)) changes very differently by the uniform thermal spreading in diffusion (in (**b**)) and the separation caused by an electric field (in (**c**))

conditions for a given ion. In steady state, the net flow of ions into any region is zero, so $J_{\rm diff} + J_{\rm elect} = 0$ and using (7.51) and (12.17) we see that

$$D_{\rm diff}\frac{{\rm d}n}{{\rm d}x} = n\mu E. \tag{12.18}$$

(In steady state n does not depend on time, so the partial derivative in (7.51) is not needed here.)

The diffusion coefficient, $D_{\rm diff}$, and mobility, μ, are actually closely related. Consider a cylinder of cross-sectional area A and length ${\rm d}x$ along the x direction than contains a density n of ions of charge q. When an electric field E is applied along the x direction, the ions in the cylinder feel a force $(nq)(A{\rm d}x)E$, where nq is the total charge per unit volume and $A{\rm d}x$ is the volume. The mechanical force on this cylinder is due to the difference between the pressure × area on one side wall, $AP(x)$, and that on the other side wall, $AP(x + {\rm d}x) = A[P(x) + ({\rm d}P/{\rm d}x){\rm d}x]$, or $-A({\rm d}P/{\rm d}x){\rm d}x$. The sum of these forces is zero in steady state, so ${\rm d}P/{\rm d}x = nqE$. Using the ideal gas law (7.2) $P = nk_{\rm B}T$ (which is an approximation here and where n is now the number of molecules per unit volume because $k_{\rm B}$ is used instead of the gas constant R), we see that ${\rm d}P/{\rm d}x = k_{\rm B}T({\rm d}n/{\rm d}x)$ or $k_{\rm B}T({\rm d}n/{\rm d}x) = nqE$. Comparing this to (12.18), gives the Einstein equation

$$\mu = \frac{qD_{\rm diff}}{k_{\rm B}T}, \tag{12.19}$$

a result we will use soon.

Now let us consider the charge current due to two ions, one of charge q (which we will say is >0), with density n_+ and mobility μ_+, and the other of charge $-q$, with density n_- and mobility μ_-. (We will now define the mobilities as being positive, so for this negative ion $v_{\rm drift} = -\mu_- E$.) If these are the only two ions, charge neutrality gives $n_+ = n_- = n$. The particle flux of each is determined by the concentration gradient of each and the motion of each in an electric field. The $j_{\rm flux}$ charge flux (or current density) is the ion charge × the ion flux. For the positive ion: $j_{{\rm flux},+} = q(J_{{\rm diff},+} + J_{{\rm elect},+}) = -qD_{{\rm diff},+}({\rm d}n/{\rm d}x) + qn\mu_+ E$ and for the negative ion it is: $j_{{\rm flux},-} = -q(J_{{\rm diff},-} + J_{{\rm elect},-}) = qD_{{\rm diff},-}({\rm d}n/{\rm d}x) + qn\mu_- E$, so the total current density is

$$j_{\rm flux} = -q(D_{{\rm diff},+} - D_{{\rm diff},-})\frac{{\rm d}n}{{\rm d}x} + qn(\mu_+ + \mu_-)E, \tag{12.20}$$

which is known as the *Nernst-Planck equation*. This can also be written as

$$j_{\rm flux} = qn(\mu_+ + \mu_-)\left(E - \frac{D_{{\rm diff},+} - D_{{\rm diff},-}}{\mu_+ + \mu_-}\,\frac{{\rm d}\ln n}{{\rm d}x}\right), \tag{12.21}$$

where we have expressed $({\rm d}n/{\rm d}x)/n$ as ${\rm d}\ln n/{\rm d}x$. The prefactor on the right-hand side is the conductivity, $\sigma = qn(\mu_+ + \mu_-)$. (Also, the factor $\Lambda_{0,i}$ in (12.15) clearly equals $q_i\mu_i$.)

When there is no net current flow, we see

$$E = \frac{D_{\text{diff},+} - D_{\text{diff},-}}{\mu_+ + \mu_-} \frac{\mathrm{d} \ln n}{\mathrm{d}x}. \tag{12.22}$$

So, the voltage between two points, such as from the inside (with subscript i) of the membrane to the outside (with subscript o) is

$$\Delta V = V_{\text{i}} - V_{\text{o}} = -\int_{\text{outside}}^{\text{inside}} E \, \mathrm{d}x \tag{12.23}$$

$$= -\frac{D_{\text{diff},+} - D_{\text{diff},-}}{\mu_+ + \mu_-} \int_{\text{outside}}^{\text{inside}} \frac{\mathrm{d} \ln n}{\mathrm{d}x} \, \mathrm{d}x \tag{12.24}$$

$$= -\frac{D_{\text{diff},+} - D_{\text{diff},-}}{\mu_+ + \mu_-} \ln(n_{\text{i}}/n_{\text{o}}). \tag{12.25}$$

Using the Einstein relation, (12.19), we know that $D_{\text{diff}} = \mu k_{\text{B}} T/q$, and so

$$\Delta V = -\frac{k_{\text{B}} T}{q} \frac{\mu_+ - \mu_-}{\mu_+ + \mu_-} \ln(n_{\text{i}}/n_{\text{o}}). \tag{12.26}$$

This is the *Nernst equation*.

Let us apply this to a membrane that is impermeable to negative ions, so $\mu_- = 0$ and

$$\Delta V = -\frac{k_{\text{B}} T}{q} \ln(n_{\text{i}}/n_{\text{o}}). \tag{12.27}$$

Calling the charge $q = Ze$, where e is the magnitude of an elementary charge (electron or proton), we see that

$$\frac{n_{\text{i}}}{n_{\text{o}}} = \exp\left(-Ze(V_{\text{i}} - V_{\text{o}})/k_{\text{B}} T\right). \tag{12.28}$$

This ratio is known as the Donnan ratio and this is known as *Donnan equilibrium*. The ion densities are considered constant within both the inside and outside regions.

This expression can also be derived by using the Maxwell–Boltzmann distribution, which gives the probability of a state being occupied, $P(E, T)$, if it has an energy E and is in thermal equilibrium with the environment at temperature T

$$P(E, T) = A \exp(-E/k_{\text{B}} T). \tag{12.29}$$

The potential energy of the charge is $E = ZeV$. If a given species were in thermal equilibrium we would expect that its concentration n would be proportional to $\exp(-ZeV_{\text{local}}/k_{\text{B}} T)$, where V_{local} is the local potential, or more exactly

$$n = n_\infty \exp(-ZeV_{\text{local}}/k_{\text{B}} T), \tag{12.30}$$

where n_∞ is the concentration very far away, where the potential is zero. In particular, we would expect the ratio of the concentrations for each ion inside and outside the cell gives (12.28).

This Donnan ratio includes the physics of the first two driving forces explained earlier, as well as the physics of thermal equilibration. For the resting potential $V_\mathrm{i} - V_\mathrm{o} = -70\,\mathrm{mV}$ at $T = 310\,\mathrm{K}$ (core body temperature) and $Z = +1$, we expect $n_\mathrm{i}/n_\mathrm{o} = 13.7$ for this "Donnan" equilibrium; for Na^+ this ratio is $15/145 = 0.103$ and for K^+ it is $150/5 = 30$. For $Z = -1$ we expect $n_\mathrm{i}/n_\mathrm{o} = 1/13.7 = 0.073$; for Cl^- this ratio is $9/125 = 0.072$ and for miscellaneous singly negative charge ions it is $156/30 = 5.2$. There is relatively good agreement for K^+ and Cl^-, and great disagreement for Na^+ and the Misc.$^-$ for the reasons given earlier, such as the Na^+ pump for Na^+. (The agreement is not perfect for K^+ because the Na^+ pump brings K^+ into the cell.)

The theoretical *Nernst potential* V_Nernst is the potential that would lead to the observed concentration ratios

$$\left(\frac{n_\mathrm{i}}{n_\mathrm{o}}\right)_\mathrm{observed} = \exp(-ZeV_\mathrm{Nernst}/k_\mathrm{B}T). \tag{12.31}$$

For Na^+ it is 61 mV, for K^+ it is $-91\,\mathrm{mV}$, and for Cl^- it is $-70\,\mathrm{mV}$.

When the Nernst equation (12.27) is generalized to include the effects of many ions, such as Na^+, K^+, and Cl^-, and membrane permeability, the *Goldman Voltage equation* is obtained

$$\Delta V = -\frac{k_\mathrm{B}T}{q}\ln\frac{p_\mathrm{Na}n_\mathrm{Na,i} + p_\mathrm{K}n_\mathrm{K,i} + p_\mathrm{Cl}n_\mathrm{Cl,i}}{p_\mathrm{Na}n_\mathrm{Na,o} + p_\mathrm{K}n_\mathrm{K,o} + p_\mathrm{Cl}n_\mathrm{Cl,o}}, \tag{12.32}$$

with membrane permeabilities p (and with the subscripts i for inside and o for outside). For neurons and sensory cells the permeability for Cl^- is so small that it can often be neglected, and we find:

$$\Delta V = -\frac{k_\mathrm{B}T}{q}\ln\frac{p_\mathrm{Na}n_\mathrm{Na,i} + p_\mathrm{K}n_\mathrm{K,i}}{p_\mathrm{Na}n_\mathrm{Na,o} + p_\mathrm{K}n_\mathrm{K,o}} \tag{12.33}$$

or

$$\Delta V = -\frac{k_\mathrm{B}T}{q}\ln\frac{\alpha n_\mathrm{Na,i} + n_\mathrm{K,i}}{\alpha n_\mathrm{Na,o} + n_\mathrm{K,o}}, \tag{12.34}$$

with $\alpha = p_\mathrm{Na}/p_\mathrm{K}$. Using the earlier concentrations and $\alpha = 0.02$, this resting potential difference is $-75\,\mathrm{mV}$, which is closer to the real resting potential than $V_\mathrm{Nernst} = -91\,\mathrm{mV}$ for K^+.

Poisson–Boltzmann Equation (Advanced Topic)

So far we have determined the concentration ratios for a given potential. A more general problem, and one that is a bit beyond our scope, is to determine the potential V by using (12.1) and (12.3) and the densities of charges in

the region. In other words, we also need to couple the potential with the distributions of ions.

By integrating the field over a surface **a**, such as a sphere, around the charge q, Coulomb's Law (12.1) becomes Gauss' Law

$$\int \mathbf{E} \cdot \mathrm{d}\mathbf{a} = \frac{1}{\epsilon_0 \epsilon}\, q. \tag{12.35}$$

This can be converted into the differential form

$$\nabla \cdot \mathbf{E} = \frac{1}{\epsilon_0 \epsilon}\, \rho, \tag{12.36}$$

where ρ is the charge density

$$\rho = \sum_i Z_i e n_i. \tag{12.37}$$

In one-dimension, this form of Gauss' Law becomes

$$\frac{\mathrm{d}E}{\mathrm{d}x} = \frac{1}{\epsilon_0 \epsilon}\, \rho. \tag{12.38}$$

Using the relation between electric field and potential (12.4) and (12.5) these become Poisson's equation

$$\nabla^2 V = -\frac{1}{\epsilon_0 \epsilon}\, \rho, \tag{12.39}$$

which in one-dimension becomes:

$$\frac{\mathrm{d}^2 V}{\mathrm{d}x^2} = -\frac{1}{\epsilon_0 \epsilon}\, \rho. \tag{12.40}$$

Combining this with the Maxwell–Boltzmann relation (12.30) and with (12.37) gives the Poisson–Boltzmann equation:

$$\nabla^2 V = -\frac{1}{\epsilon_0 \epsilon} \sum_i Z_i e n_{i,0} \exp(-Z_i e V / k_\mathrm{B} T). \tag{12.41}$$

Without these free and mobile charges in solution, the potential from a charge Ze, such as an ion in solution, is given by (12.2), $V = Ze/4\pi\epsilon_0 \epsilon r$. These mobile charges partially *screen* or *shield* the potential due to this charge, as is seen by solving the Poisson–Boltzmann equation. When $Z_i e V / k_\mathrm{B} T \ll 1$, we can use $\exp(1 + x) \simeq 1 + x$ for $\mid x \mid \ll 1$ to approximate the exponential in (12.41) as $1 - Z_i e V / k_\mathrm{B} T$. This gives

$$\nabla^2 V = -\frac{1}{\epsilon_0 \epsilon} \sum_i Z_i e n_{i,0} + \frac{1}{\epsilon_0 \epsilon} \sum_i \frac{Z_i^2 e^2 n_{i,0} V}{k_\mathrm{B} T}. \tag{12.42}$$

In charge neutral regions the first term on the right-hand side sums to zero, leaving

$$\nabla^2 V = \frac{e^2}{\epsilon_0 \epsilon k_{\mathrm{B}} T} \left(\sum_i Z_i^2 n_{i,0} \right) V \tag{12.43}$$

or

$$\nabla^2 V = \kappa^2 V, \tag{12.44}$$

where κ is the Debye–Huckel parameter given by

$$\kappa^2 = \frac{e^2}{\epsilon_0 \epsilon k_{\mathrm{B}} T} \sum_i Z_i^2 n_{i,0} \tag{12.45}$$

This is solved in three-dimensions (see Problem 12.8 and Appendix C) to obtain the potential

$$V(r) = \frac{Ze}{4\pi\epsilon_0 \epsilon r} \exp(-\kappa r). \tag{12.46}$$

This means the charge is shielded beyond the Debye–Huckel length given by the radius $1/\kappa$.

12.3.2 Types of Cell Membrane Excitations

There are two qualitatively different types of axon excitations: graded potentials and action potentials.

Graded potentials (Fig. 12.14) are minor perturbations in the membrane potential due to the binding of neurotransmitters, the stimulation of sensory

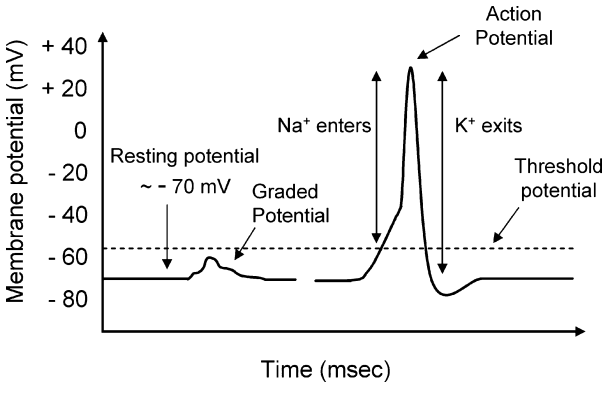

Fig. 12.14. The (subthreshold) graded potentials and (above threshold) action potentials

reception, or spontaneous ion leakage through the cell membrane. There is no threshold needed to stimulate a graded potential. They last for 5 ms to several min. Graded potentials can be either membrane depolarizations or hyperpolarizations. Successive graded potentials can add to one another. They propagate only short distances along the membrane before they decay.

Action potentials are qualitatively different from graded potentials in every way (Fig. 12.14). They initially have relatively large depolarizations by ∼15–20 mV above the resting value of −70 mV to a threshold of about ∼ −55 mV. At this threshold potential the cell membrane opens up allowing Na^+ transport. The potential lasts for 1–5 ms, and it always involves depolarization of the membrane. Each action potential opens the cell membrane, and they do not add to one another. There is no decrease in potential along the entire length of the neuron cell axon, as this action potential leads to propagation of an electrical signal along the axon. We will analyze this quantitatively in Sect. 12.3.3.

Figure 12.14 shows the time sequence of the action potential at one point in the axon. After the threshold of ∼ −55 mV is reached, the voltage-gated Na^+ channels begin to open and Na^+ rushes into the cell due to the negative potential. There is an overshoot of positive ions inside the cell and the potential becomes positive, increasing to ∼20 mV. This causes positive ions, such as K^+, to leave the cell and the potential decreases below the threshold potential to the resting potential (which is an overshoot). This electrical pulse travels along the axon. Figure 12.15 shows the depolarization and repolarization and the flow of ions for cardiac muscle. The local motion of ions near the membrane are shown in Fig. 12.16 during signal propagation.

12.3.3 Model of Electrical Conduction along an Axon

Neural axons can be treated as an electrical cable with passive parameters that characterize it per unit length, with one striking exception. The resistance of the fluids inside the axon, r_i, outside the axon, r_o, and of the axon membrane, r_m, can be characterized per unit length of the axon. The axon can also be characterized by its capacitance per unit length, c_m. The axon can then be modeled by the electrical cable in Fig. 12.17 with repeating units. So far, this description can explain only the decaying features of graded potentials. As we will see, the propagation of action potentials along the axon requires the additional current flow of ions across the axon membrane (see [569, 581, 582, 586]).

Properties of Neurons and Nerves

The parameters in Table 12.5 for unmyelinated and myelinated nerve axons will help us understand the electrical properties of the axon as we would any cable with a distributed resistance and capacitance. From Table 12.5, the resistivity for an unmyelinated nerve is typically $\rho_\mathrm{i} = 0.5$ ohm-m and the axon

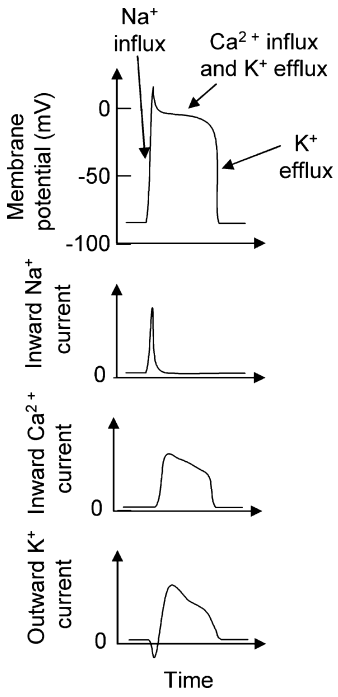

Fig. 12.15. The depolarization and repolarization of cardiac muscle, along with the flows of Na^+, Ca^{2+}, and K^+ ions. The inward flux of Na^+ and Ca^{2+} increases the potential and the outward flux of K^+ decreases it. (Based on [585])

radius is $a = 5 \times 10^{-6}$ m, and so the resistivity inside the axon per unit length along the axon is

$$r_{\mathrm{i}} = \frac{\rho_{\mathrm{i}}}{\pi a^2} = \frac{0.5 \text{ ohm-m}}{\pi(5 \times 10^{-6} \text{ m})^2} = 6.4 \times 10^9 \text{ ohm/m} = 6.4 \times 10^3 \text{ ohm/}\mu\text{m}. \tag{12.47}$$

The resistivity of the membrane is $\rho_{\mathrm{m}} = 1.6 \times 10^7$ ohm-m, the membrane thickness is $b = 6 \times 10^{-9}$ m, and the cross-sectional area of the membrane normal to the axon axis is $A = 2\pi ab$. Therefore, the membrane resistivity per unit length along the axon is

$$r_{\mathrm{m}} = \frac{\rho_{\mathrm{m}}}{2\pi ab} = \frac{1.6 \times 10^7 \text{ ohm-m}}{2\pi(5 \times 10^{-6} \text{ m})(6 \times 10^{-9} \text{ m})} \tag{12.48}$$

$$= 8 \times 10^{19} \text{ ohm/m} = 8 \times 10^{13} \text{ ohm/}\mu\text{m}, \tag{12.49}$$

This resistivity is so high that for a given voltage drop along the axon, the current flow along the membrane is negligible compared to that in the fluid.

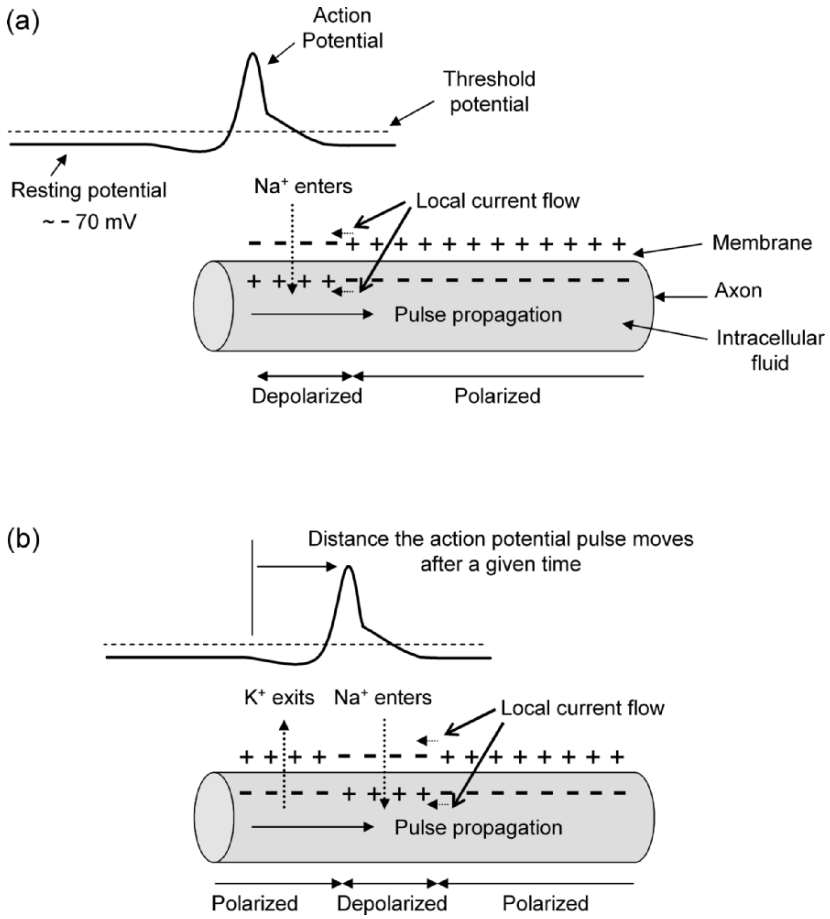

Fig. 12.16. The flow of ions across the membrane during action potential propagation (**a**) at a given time and (**b**) at a later time

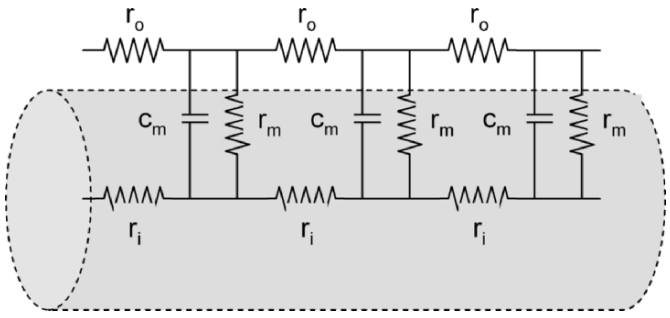

Fig. 12.17. Distributed circuit model of an axon, with resistance inside the axon r_i, membrane resistance r_m and capacitance c_m, and resistance outside the axon r_o, each per unit length

Table 12.5. Typical parameters for unmyelinated and myelinated nerves. (From [570, 571, 581])

		unmyelinated	myelinated
axon inner radius (m)	a	5×10^{-6}	5×10^{-6}
membrane/myelin thickness (m)	b	6×10^{-9}	2×10^{-6}
axoplasm resistivity (ohm-m)	ρ_{i}	1.1	1.1
membrane dielectric constant (s/ohm-m)	$\kappa\epsilon_0$	6.20×10^{-11}	6.20×10^{-11}
membrane/myelin resistivity (ohm-m)	ρ_{m}	10^7	10^7
resistance per unit length of fluid[a] (ohm/m)	r	6.37×10^9	6.37×10^9
conductivity/length axon membrane (mho/m)	g_{m}	1.25×10^4	3×10^{-7}
capacitance/length axon (F/m)	c_{m}	3×10^{-7}	8×10^{-10}

[a]Fluid both inside and outside the axon.

The transverse resistance across the membrane is $(\rho_{\mathrm{m}}b)A_{\mathrm{transverse}}$, so the conductance per unit area is

$$g_{\mathrm{m}} = \frac{1}{\rho_{\mathrm{m}}b}, \tag{12.50}$$

where conductance is the reciprocal of the resistance.

Because the axon radius a of an unmyelinated axon is much greater than the membrane thickness b, the cylindrical membrane can be unrolled along its length (much as in Fig. 8.23) and modeled very successfully as a plane parallel capacitor, with plate separation b and area $A = aL$, where L is the length of the axon unit. The material in the axon membrane has dielectric constant $\kappa = 7$, so with $\epsilon_0 = 8.85 \times 10^{-12}$ s/ohm-m, we see that $\kappa\epsilon_0 = 6.20 \times 10^{-11}$ s/ohm-m. From (12.13), the capacitance per unit length of an unmyelinated axon is

$$C_{\text{parallel plates,per length}} = C_{\text{parallel plates}}/L = \kappa\epsilon_0 a/b \tag{12.51}$$

$$= (6.20 \times 10^{-11}\text{s/ohm-m})(5 \times 10^{-6}\text{m})/6 \times 10^{-9}\text{m} \tag{12.52}$$

$$= 3 \times 10^{-7}\ \text{F/m} \tag{12.53}$$

and that per unit area is

$$c_{\text{parallel plates}} = C_{\text{parallel plates}}/La = \kappa\epsilon_0/b \tag{12.54}$$

$$= (6.20 \times 10^{-11}\text{s/ohm-m})/6 \times 10^{-9}\ \text{m} \tag{12.55}$$

$$= 0.01\ \text{F/m}^2. \tag{12.56}$$

Using (12.12), $q = CV$ and the charge density on the membrane walls is $\sigma = q/A = (C/A)/V$. For a -70 mV voltage drop, we see that $\sigma = (C/A)/V = (0.01\,\text{F/m}^2)(70\,\text{mV}) = 7 \times 10^{-4}\,\text{C/m}^2$. Because an elementary charge is

1.6×10^{-19} C, there are $(7\times10^{-4})(6.25\times10^{18}$ elementary charges$)/10^{12}$ μm^2 = 4.4×10^3 elementary charges/μm^2.

Does the flow of Na ions through the open ion channels appreciably affect the total number of such ions in the axon? This open channel corresponds to a voltage change from −70 to 30 mV or about 100 mV. Using the analysis of the previous paragraph, this corresponds to a change in charge of 6×10^3 elementary charges/μm^2. Consider a 1 μm long section of the axon. Its inner area is $2\pi(5\ \mu\text{m})(1\ \mu\text{m}) = 31\ \mu\text{m}^2$, so 2×10^5 Na^+ ions are transported into this volume, because they each have one elementary charge. Before the membrane opened there were 15 mmol/L of Na^+ ions inside the membrane, or $[(15 \times 6.02 \times 10^{20})/10^{15}\ \mu\text{m}^3][\pi(5\ \mu\text{m})^2(1\ \mu\text{m})] = 7 \times 10^8$ Na^+ ions in this volume (and, similarly, 7×10^9 K^+ ions inside this volume). This means that this Na^+ ion transport increases the density by only about 0.03%. (Large changes in potentials are often caused by the transfer of very few charges!)

Model of Electrical Conduction in Axons (Advanced Topic)

Several things can happen when you apply a voltage to an axon of a neuron. There can be current flow of charged ions associated with the resistance in and about the axon; the voltage would drop with distance according to Ohm's Law and there would be dissipation of energy. There can be motion of charges to and from axon membranes and changes in the electric field energy stored between these charged surfaces, as characterized by their capacitance. There can also be changes in the transport of charges through these axon membranes.

Consider a cylindrical "pillbox" as shown in Fig. 12.18 of radius a and length δx, extending from x to $x + \delta x$ along the axon and with the curved cylinder surface within the cell membrane itself. The voltage at x is $V(x)$ and that at $x + \delta x$ is $V(x + \delta x)$. The current flowing (due to ions) within the axoplasm – i.e., the medium inside the axon – into this volume is $I_i(x)$ and that leaving it is $I_i(x + \delta x)$. There is a charge $+q$ on the outer membrane of the axon and a charge $-q$ on the inner membrane wall. A physical model for this is shown in Fig. 12.19.

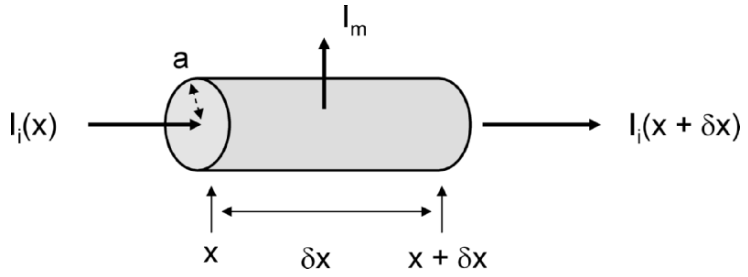

Fig. 12.18. Longitudinal current in an axon, with a "pillbox" for examining current flow, including the membrane current. (Based on [581])

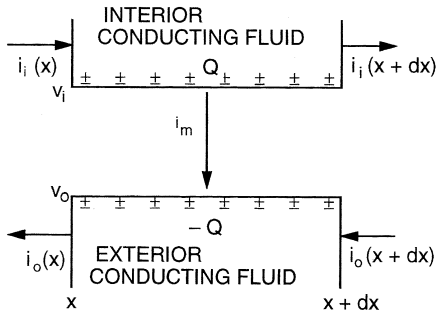

Fig. 12.19. A more physical model for the axon currents shown in Fig. 12.18. (From [581])

We will apply Kirchhoff's 1st Law (12.8) to this construct and sum all currents entering this pillbox. There are current flows inside the axon $I_{\mathrm{i}}(x)$ and $-I_{\mathrm{i}}(x+\delta x)$ entering the pillbox. There is also a current flow due to the flow of ions across the cell membrane I_{m}. We will say it is positive when it leaves the axon (Fig. 12.18), so $-I_{\mathrm{m}}$ enters it. The voltage across the cell membrane $V = q/C_{\mathrm{m}}$, where C_{m} is membrane capacitance. The time rate of change of the voltage is related to another current I_{c} associated with the change of charge on the cell membrane walls

$$\frac{\mathrm{d}V}{\mathrm{d}t} = \frac{\mathrm{d}q/\mathrm{d}t}{C_{\mathrm{m}}} = \frac{I_{\mathrm{c}}}{C_{\mathrm{m}}} \tag{12.57}$$

or

$$I_{\mathrm{c}} = C_{\mathrm{m}}\frac{\mathrm{d}V}{\mathrm{d}t}. \tag{12.58}$$

I_{c} flows to the outside, so $-I_{\mathrm{c}} = -C_{\mathrm{m}}(\mathrm{d}V/\mathrm{d}t)$ flows into the axon. Kirchhoff's 1st Law gives

$$I_{\mathrm{i}}(x) - I_{\mathrm{i}}(x+\delta x) - I_{\mathrm{m}} - C_{\mathrm{m}}\frac{\mathrm{d}V}{\mathrm{d}t} = 0 \tag{12.59}$$

or

$$I_{\mathrm{i}}(x) - I_{\mathrm{i}}(x+\delta x) - I_{\mathrm{m}} = C_{\mathrm{m}}\frac{\mathrm{d}V}{\mathrm{d}t}. \tag{12.60}$$

Using $I_{\mathrm{i}}(x+\delta x) \simeq I_{\mathrm{i}}(x) + (\mathrm{d}I_{\mathrm{i}}/\mathrm{d}x)\delta x$, we see that $I_{\mathrm{i}}(x) - I_{\mathrm{i}}(x+\delta x) \simeq -(\mathrm{d}I_{\mathrm{i}}/\mathrm{d}x)\delta x$ and this equation becomes

$$-\frac{\mathrm{d}I_{\mathrm{i}}}{\mathrm{d}x}\delta x - I_{\mathrm{m}} = C_{\mathrm{m}}\frac{\mathrm{d}V}{\mathrm{d}t}. \tag{12.61}$$

Using Ohm's Law, the voltage drop across the pillbox is

$$V(x) - V(x+\delta x) = I_{\mathrm{i}}(x) r_{\mathrm{i}}(\delta x), \tag{12.62}$$

where the resistance is $R_\mathrm{i} = r_\mathrm{i}\delta x$. Because $V(x+\delta x) \simeq V(x) + (\mathrm{d}V/\mathrm{d}x)\delta x$, we see that $V(x) - (V(x) + (\mathrm{d}V/\mathrm{d}x)\delta x) \simeq I_\mathrm{i}(x) r_\mathrm{i}(\delta x)$ or

$$I_\mathrm{i}(x) = -\frac{1}{r_\mathrm{i}}\frac{\mathrm{d}V}{\mathrm{d}x}. \tag{12.63}$$

Taking the first derivative of both sides gives $\mathrm{d}I_\mathrm{i}/\mathrm{d}x = -(1/r_\mathrm{i})\mathrm{d}^2V/\mathrm{d}x^2$, and (12.61) becomes

$$\frac{1}{r_\mathrm{i}}\frac{\mathrm{d}^2V}{\mathrm{d}x^2}(\delta x) - I_\mathrm{m} = C_\mathrm{m}\frac{\mathrm{d}V}{\mathrm{d}t}. \tag{12.64}$$

Dividing both sides by the membrane surface area is $(2\pi a)(\delta x)$ gives

$$\frac{1}{2\pi a r_\mathrm{i}}\frac{\mathrm{d}^2V}{\mathrm{d}x^2} - \frac{I_\mathrm{m}}{(2\pi a)\delta x} = \frac{C_\mathrm{m}}{2\pi a(\delta x)}\frac{\mathrm{d}V}{\mathrm{d}t}. \tag{12.65}$$

With the membrane current density (membrane current per unit area) defined as $J_\mathrm{m} = I_\mathrm{m}/(2\pi a(\delta x))$ and the membrane capacitance per unit area expressed as $c_\mathrm{m} = C_\mathrm{m}/(2\pi a(\delta x))$, this becomes

$$\frac{1}{2\pi a r_\mathrm{i}}\frac{\mathrm{d}^2V}{\mathrm{d}x^2} - J_\mathrm{m} = c_\mathrm{m}\frac{\mathrm{d}V}{\mathrm{d}t} \tag{12.66}$$

or

$$c_\mathrm{m}\frac{\partial V(x,t)}{\partial t} = -J_\mathrm{m} + \frac{1}{2\pi a r_\mathrm{i}}\frac{\partial^2 V(x,t)}{\partial x^2}. \tag{12.67}$$

This has now been expressed in terms of partial derivatives with respect to t and x, which means that the derivatives are taken with respect to t and x, respectively, treating x and t as constants. Also, the voltage is explicitly written as a function of x and t.

How do we treat active charge transport across the membrane? We model the membrane current as being $g_\mathrm{i}(V - V_i)$ for each ion, with g_i the conductance per unit area and V_i a characteristic voltage being parameters for the specific ion. The total membrane current is

$$J_\mathrm{m} = \sum_i g_i(V - V_i) = g_\mathrm{Na}(V - V_\mathrm{Na}) + g_\mathrm{K}(V - V_\mathrm{K}) + g_\mathrm{L}(V - V_\mathrm{L}), \tag{12.68}$$

where we have included conduction by Na^+ and K^+ ions and by other ions (leakage, L). This *Hodgkin-Huxley model* is depicted in Fig. 12.20. So we find

$$c_\mathrm{m}\frac{\partial V(x,t)}{\partial t} = -\sum_i g_i(V(x,t) - V_i) + \frac{1}{2\pi a r_\mathrm{i}}\frac{\partial^2 V(x,t)}{\partial x^2} \tag{12.69}$$

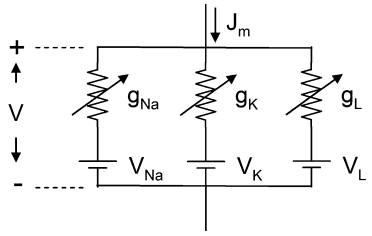

Fig. 12.20. Equivalent circuit of the Hodgkin-Huxley model of the membrane current, with variable resistors g_i and voltage sources V_i. (Based on [581])

or for only one ion

$$c_{\mathrm{m}}\frac{\partial V(x,t)}{\partial t} = -g_i(V(x,t) - V_i) + \frac{1}{2\pi a r_{\mathrm{i}}}\frac{\partial^2 V(x,t)}{\partial x^2}. \tag{12.70}$$

This last equation is known as the *Cable or Telegrapher's equation* because it also describes the propagation of electrical signals along long cables, such as submarine cables, as well as the propagation of such signals along axons in neurons. Remember that although the voltage disturbance propagates long distances, the charges move very little and in fact they move essentially only across the membrane wall, which is normal to the direction of wave propagation. (By the way, John Carew Eccles, Alan Lloyd Hodgkin, and Andrew Fielding Huxley shared the Nobel Prize in Physiology or Medicine in 1963 for their discoveries concerning the ionic mechanisms involved in excitation and inhibition in the peripheral and central portions of the nerve cell membrane, which are part of this Hodgkin-Huxley model.)

When this wave propagates at a speed u it travels as a pulse (Fig. 12.21) with unchanging shape that has constant $x - ut$. (See the discussion of sound wave propagation in Chap. 10.) It can then be shown that $\partial^2 V/\partial t^2 = u^2\partial^2 V/\partial x^2$ or $\partial^2 V/\partial x^2 = (1/u^2)\partial^2 V/\partial t^2$ and so (12.70) can be written in terms of only derivatives with respect to time. Including the three ions, we see that:

$$\frac{1}{2\pi a r_{\mathrm{i}} u^2}\frac{\partial^2 V}{\partial t^2} - c_{\mathrm{m}}\frac{\partial V}{\partial t} = g_{\mathrm{Na}}(V - V_{\mathrm{Na}}) + g_{\mathrm{K}}(V - V_{\mathrm{K}}) + g_{\mathrm{L}}(V - V_{\mathrm{L}}) \tag{12.71}$$

with typical neuron properties given in Table 12.5. More details can be found in [581, 586].

Propagation Speed for Action Potentials

These equations must be solved numerically. Still we can gain some insight concerning the speed of these electrical signals along the axon by using an

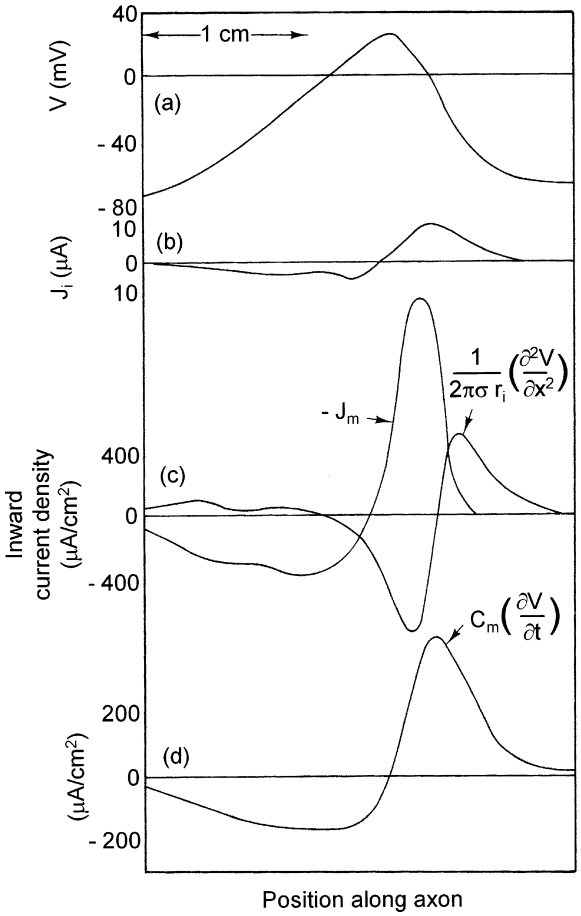

Fig. 12.21. A snapshot of the (**a**) voltage and (**b**) axon current of the pulse propagating along an axon; (**c**) current densities corresponding to the two terms on the right-hand side of (12.67); (**d**) current charging or discharging of the membrane. They are all calculated using (12.67). (From [581])

analytical method. Using (12.47), (12.50), and (12.54), we can rearrange (12.70) to give

$$\lambda^2 \frac{\partial^2 V(x,t)}{\partial x^2} - V(x,t) - \tau \frac{\partial V(x,t)}{\partial t} = -V_i, \tag{12.72}$$

where

$$\lambda = \sqrt{\frac{1}{2\pi a r_{\mathrm{i}} g_i}} = \sqrt{\frac{ab\rho_{\mathrm{m}}}{2\rho_{\mathrm{i}}}} \tag{12.73}$$

and

$$\tau = \frac{c_{\mathrm{m}}}{g_i} = \kappa\varepsilon_0\rho_{\mathrm{m}}. \tag{12.74}$$

We see that λ has units of distance and τ has units of time in (12.72), so it is not unreasonable to think that the conduction speed u is approximately

$$u \sim \frac{\lambda}{\tau} = \sqrt{\frac{ab}{2\rho_{\mathrm{i}}\rho_{\mathrm{m}}}}\,\frac{1}{\kappa\varepsilon_0}. \tag{12.75}$$

For an unmyelinated axon $b \approx 6\,\mathrm{nm}$ and so using the parameters in Table 12.5, we find

$$u_{\mathrm{unmyelinated}} \sim 0.27\sqrt{a}, \tag{12.76}$$

where u is in m/s and a is in μm. This is about 7× slower than observed, namely $1.8\sqrt{a}$.

For a myelinated axon, $b \approx 0.4a$, so $\lambda = 1,350a$ and

$$u_{\mathrm{myelinated}} \sim 2.2a, \tag{12.77}$$

which is again about 7× slower than observed, namely $17a$. This conduction model with Hodgkin-Huxley-type conduction across the membrane is not expected to be very accurate because, unlike that of the bare membrane, the conduction of the myelin sheath is independent of the voltage. Therefore, propagation occurs in the sheath region with this term and there is some decay until the signal reaches the next node of Ranvier. The signal is regenerated at this sheath-free membrane and then propagates until the next regeneration stage. If we instead assumed in the model of conduction in myelinated axons that the conduction speed is $u_{\mathrm{myelinated}} \sim D/\tau$, where $D \approx 280a$ is the distance between Ranvier nodes, the model conduction speed would be

$$u_{\mathrm{myelinated}} \sim 0.45a, \tag{12.78}$$

which is about 40× slower than observations.

The speed of nerve conduction can be measured by applying a stimulating voltage pulse at one place on the body and using electrodes to sense the time delay in the propagated pulse at another place on the body, as seen in Fig. 12.22 [568].

Passive Spreading

When voltages are below the threshold of $\sim -55\,\mathrm{mV}$, the graded potential–voltage disturbance decays along the axon and in time. We can use this model to understand this. This is equivalent to the distributed circuit model in Fig. 12.17.

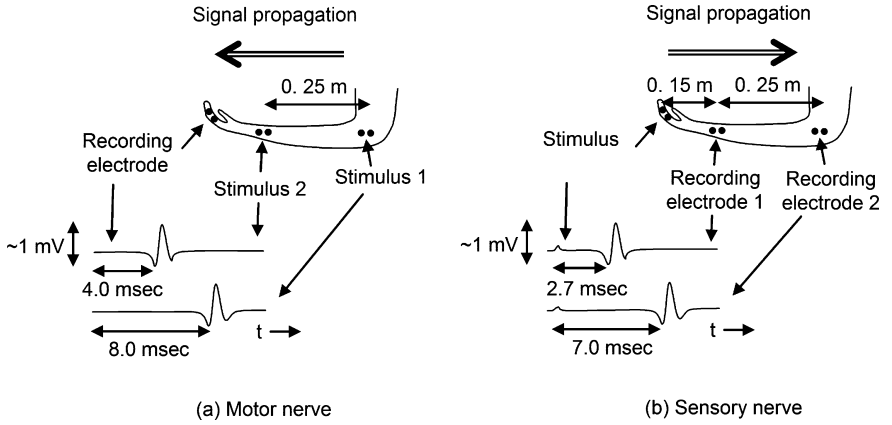

Fig. 12.22. Measuring the conduction speed along the lower arm and hand of (**a**) a motor nerve and (**b**) a sensory nerve, along with associated EMG signals. The conduction speed of the motor nerve in (a) is 62.5 m/s, and the conduction speed of the sensory nerve in (b) is 58.1 m/s (see Problem 12.18). (Based on [568])

Special Case: Only Resistance, No Capacitance, Infinitely Long Cable. If membrane capacitance is neglected in the model ($c_\mathrm{m} = 0$ and so $\tau = 0$), then (12.72) becomes

$$\lambda^2 \frac{\partial^2 V(x)}{\partial x^2} - V(x) = -V_i \tag{12.79}$$

and V does not depend on time. If at, say, $x = 0$, the voltage is held at $V = V_i + V_0$, the solution is

$$V(x) = V_i + V_0 \exp(-x/\lambda) \qquad \text{for } x > 0 \tag{12.80}$$

$$= V_i + V_0 \exp(+x/\lambda) \qquad \text{for } x < 0, \tag{12.81}$$

which can be proved by substitution. This means the subthreshold disturbance decays over a characteristic distance λ, as seen in Fig. 12.23.

Special Case: Only Resistance, No Capacitance, Cable of Finite Length. If the cable is semi-infinite or of finite length, the solution to (12.79) needs to be modified [589]. Such solutions are shown in Fig. 12.24 and are examined further in Problem 12.24 (for $V_i = 0$). Of particular importance for a cable of finite length is exactly how the axon is terminated at either end, i.e., the boundary conditions. Usually these boundary conditions are specified by giving the voltage V or the current flow (which is proportional to $\mathrm{d}V/\mathrm{d}x$) at the end of the axon cable.

Special Case: Only Resistance, No Capacitance, Infinitely Long Cable. If instead the axoplasm resistance is set equal to zero (such as by placing a wire

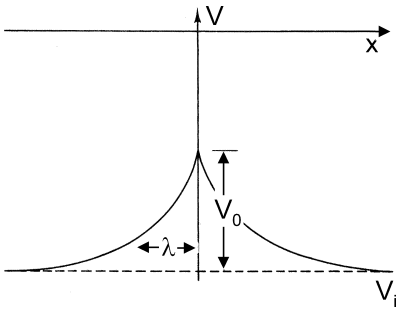

Fig. 12.23. With no axon membrane capacitance, a voltage disturbance decays over a characteristic distance λ. (From [581])

axially in the axon), then $\lambda^2(\partial^2 V(x,t)/\partial x^2) = 0$ and (12.72) becomes

$$\tau \frac{\partial V(x,t)}{\partial t} + V(x,t) = V_i. \tag{12.82}$$

(As in Fig. 12.17, transverse resistance is still possible.) If at, say, $t = 0$, the voltage were constrained to $V = V_i + V_0$ and the constraint were released, then for any x

$$V(t) = V_i + V_0 \exp(-t/\tau) \qquad \text{for } t > 0. \tag{12.83}$$

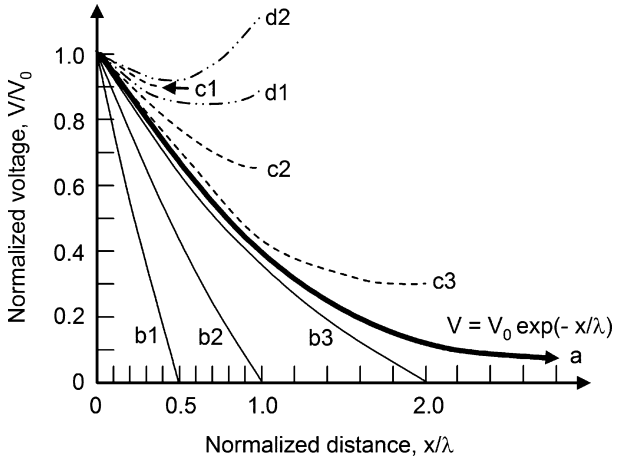

Fig. 12.24. Steady-state solutions to (12.79) for a (**a**) semi-infinite cable and (**b**)–(**e**) cables of finite length L with different boundary conditions at the end, with characteristic distance λ and $V = V_0$ at $x = 0$. For curves (b1)–(b3), $V(L) = 0$ (voltage clamped to zero), for $L = 0.5\lambda,\ \lambda$, and 2.0λ. For curves (c1)–(c3), $\mathrm{d}V/\mathrm{d}x = 0$ (current clamped to zero) at $x = L$, for $L = 0.5\lambda,\ \lambda$, and 2.0λ. For curves (d1) and (d2), the voltage is clamped to $0.9V_0$ and $1.1V_0$ at $x = L$, for $L = \lambda$. Also see Problem 12.24. (Based on [589])

Again, this can be proved by substitution. This means the subthreshold disturbance decays in a characteristic time τ.

General Case, Infinitely Long Cable. We can find a more general solution by substituting a trial solution

$$V(x,t) = V_i + w(x,t)\exp(-t/\tau), \tag{12.84}$$

into (12.72). This leads to:

$$\frac{\lambda^2}{\tau}\frac{\partial^2 w(x,t)}{\partial x^2} = \frac{\partial w(x,t)}{\partial t}. \tag{12.85}$$

This is the diffusion equation (Fick's Second Law of Diffusion, see (7.53); also see Appendix C). The disturbance w spreads in a gaussian-like manner over a distance λ in a time τ, approximately as

$$w(x,t) \propto \exp(-x^2/2D_{\text{diff}}t), \tag{12.86}$$

where the diffusion constant $D_{\text{diff}} = \lambda^2/\tau$. This assumes an initial voltage spike at $x = 0$. Using (12.84), the real voltage disturbance spreads as:

$$V(x,t) - V_i \propto \exp(-x^2/2D_{\text{diff}}t)\exp(-t/\tau), \tag{12.87}$$

which has an additional overall exponential decay in time with characteristic time τ.

12.4 Ion Channels, Hair Cells, Balance, Taste, and Smell

The previous section addressed the conduction of signals in an axon. Equally important is the actual generation of signals that are then conducted along an axon to the brain. We saw in the previous section that controlling the flow of ions across the cell membrane – by changes in the permeability of membranes to ions by the opening or closing of *ion channels* – is important in this conduction. It is also important in the generation of signals, as in sensing.

One interesting example is the excitation of hair cells, which is important in several parts of the body. Figure 12.25 shows that the "hair" in a hair cell is a hair bundle composed of an asymmetric series of 20–300 *microvilli*, which become successively larger in one direction. At the end of the bundle there is often one large cilium, which is called a *kinocilium*. When the hair bundle moves toward the kinocilium, the membrane potential depolarizes relative to the resting potential and when it moves away from it, the membrane hyperpolarizes, as is seen in Fig. 12.26. There is no change in membrane potential when the bundles moves perpendicular to the direction of increasingly large microvilli. One possible explanation for this depolarization is that Na^+ positive ion channels open when the hair bundle is displaced toward the kinocilium. The elastic response of the hair cell comes from the microvilli themselves, the elastic elements (*gating springs*) that pull on the ion channels, and the

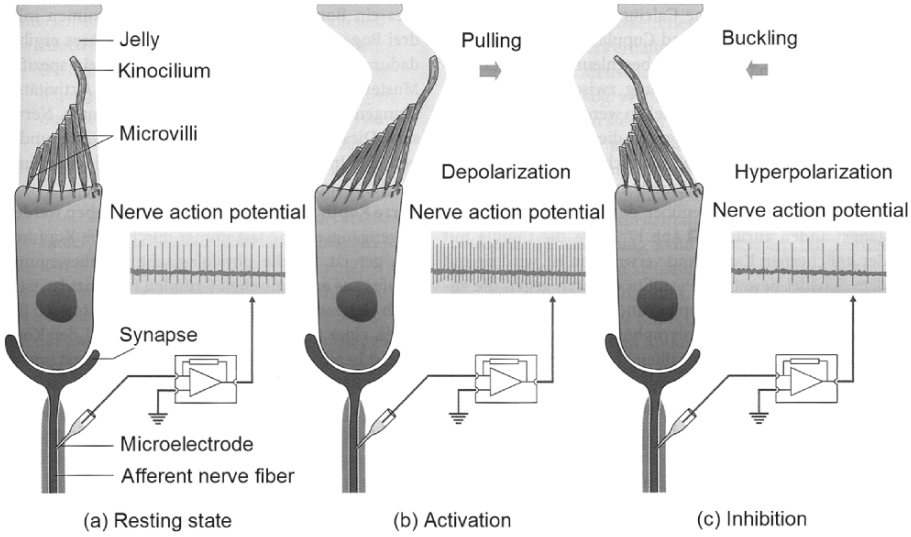

Fig. 12.25. In one mechanism for hair cell response, the hair bundle moves toward the kinocilium (hair with the bead) opening channels that are permeable to Na^+ (which is depolarization), as shown in (**b**). Resting activity is seen in (**a**) and hyperpolarization in (**c**). (From [593])

channels themselves. The response of hair to forces was discussed in Chap. 10 (text and Problem 10.55).

These hair cells are important in the ear, contributing both to the generation of auditory signals in the cochlea that travel to the brain to enable hearing and in the vestibular system in the ear that helps us maintain a sense

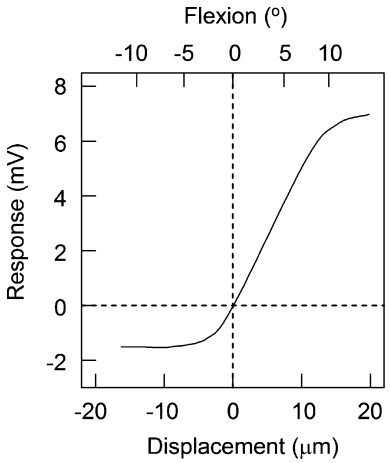

Fig. 12.26. Membrane potential vs. hair displacement (in position and angle). Positive displacements are toward the kinocilium. (Based on [574, 583])

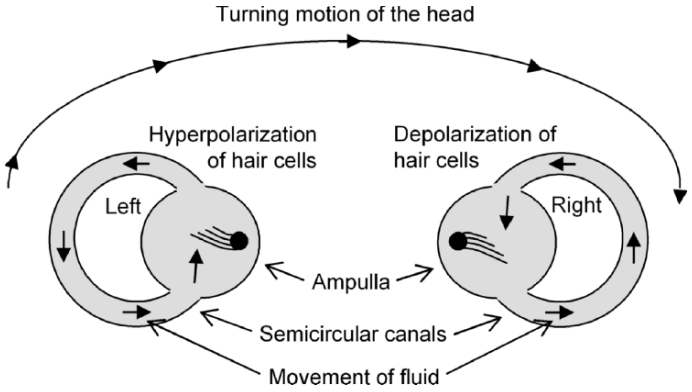

Fig. 12.27. The sense of balance is seen by examining the pair of horizontal semicircular canals, by looking at the head from above. When you turn your head clockwise there is counterclockwise motion of the cochlear fluid that depolarizes the hair cells in the semicircular canal in the right ear and hyperpolarizes them in the left ear. (Based on [574])

of balance. Each ear has three semicircular canals that are approximately orthogonal to each other, which provide us with a sense of balance through a sensing of the motion of fluid in them. Figure 12.27 shows how hair cells sense one such motion, that of turning your head to the right. This is clockwise looking from the top, as in the figure. The fluid in the two depicted horizontal semicircular canals lags behind this motion (Newton's First Law), and so it moves counterclockwise relative to the hair cells. This causes a depolarization of the hair cells in the right ear and a hyperpolarization of the hair cells in the left ear. These semicircular canals contain hair cells that are bathed in a fluid, the endolymph, which has high concentrations of K^+ and low concentrations of Na^+ and Ca^{2+}. Consequently, when the hair cells are stimulated, K^+ enters the cell through the channels during this depolarization. The hair cells in the cochlea are also bathed by this endolymph fluid in the scala media so the control of K^+ ion channels by the hair bundles is also important in hearing transduction (where transduction is the conversion of one kind of signal or stimulus into another by a cell, which in this case is the conversion of sound into an electrical signal). (The perilymph fluid in the scala vestibuli and the scala tympani is high in Na^+ and low in K^+, as are blood and cerebrospinal fluid.)

The importance of hair cells in the sense of touch (for hairy skin) was discussed in Chap. 2. The sense of touch by Merkel receptors, Meissner corpuscles, Ruffini cylinders, and Pacinian corpuscles in both hair-free and hairy skin arises from changes in the ion channels caused by applied pressure.

Taste bud sensors are found in clusters called taste buds on the tongue and other places in the oral cavity. There are several mechanisms that activate sensors of taste for sweet, sour, bitter, salty, and "umani," all involving the control of membrane ion channels. (Umani is the Japanese word for delicious. In this context it describes the taste of monosodium glutamate and other

amino acids.) The conceptually simplest is that for saltiness, which is detected by a Na^+ channel that depolarizes the detector cell.

The olfactory receptor region in the nose has an area of $\sim$1–2 cm^2, with $\sim$12 million receptor cells. (There are $\sim$4 billion such cells in a German shepherd dog.) The sense of smell is activated by olfactory neurons, with the opening of ion channels. In many such neurons, this allows Na^+ to enter the cell during depolarization, which induces an increase in the firing of action potentials.

12.5 Electrical Properties of the Heart

The total charge of the heart is zero during the heart beat, but there are dynamic separations between positive and negative charges. These create an electric dipole that rotates as it becomes larger and then smaller in magnitude during each cardiac cycle. The electric potential at different places on the skin consequently changes with time during each cycle and this is what is sensed in an electrocardiogram (EKG or ECG). These potential differences are typically $\sim$30–500 μV. Usually 12-lead scalar EKG measurements are made, which give much information about the evolution of the cardiac dipole and sufficiently valuable information concerning potential abnormalities in the heart. Vector EKGs are taken less often; they can provide a more complete view of the evolution of the heart dipole during a heart beat. A typical EKG is shown in Fig. 12.28.

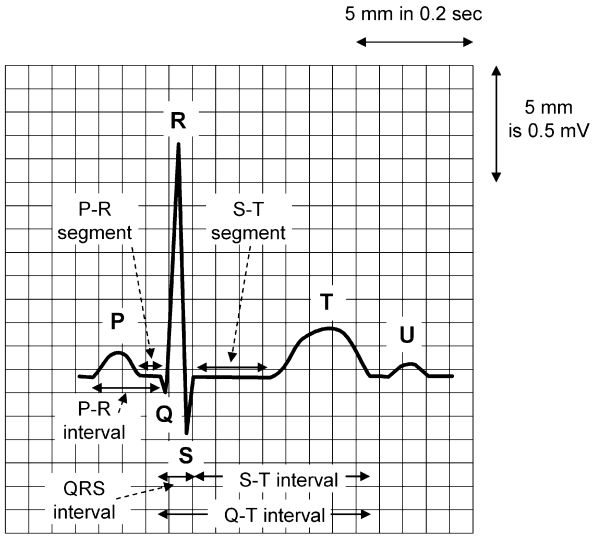

Fig. 12.28. A normal electrocardiogram (EKG/ECG), showing the P wave (atrial depolarization), QRS complex (ventricular depolarization), and T wave (ventricular repolarization) in a single cardiac cycle. Typically the scan proceeds with 25 mm/s and the signal strength is plotted as 10 mm/mV. (Based on [586])

From an electrical perspective, the heart can be described as an electric dipole whose magnitude and direction varies in a cyclic manner, repeating for each heart cycle. As for the axon described earlier in this chapter, the positions of charges in the cardiac muscle cells change during cell depolarization in muscle contraction and repolarization. This constitutes a change in the electric dipole moment of the individual cell. The electric fields due to all such heart muscle cells add to produce voltage variations in the body that are sensed by the EKG probes. The voltages vary with time indicating the depolarization (contraction) of the right and left atria (called the P wave), the depolarization (contraction) of the right and left ventricles during systole (the QRS complex) – the repolarization of the atria is masked by this, and the repolarization of the ventricles (the T wave). The time dependence can indicate normal or abnormal firing of the heart muscle, and this could, in principle, be determined from the voltage difference across two EKG probes. Analysis of the voltages across several pairs of electrodes provides important information that is used to spatially locate abnormalities in different parts of the heart muscle, such as after a heart attack. The EKG probes measure the electric potential (voltage) just below the skin. The resistance across the skin is not significant because the EKG probes are connected to the skin with a special contact jelly.

The difference in potential across the cell membrane of the cardiac muscle cell changes during the depolarization and subsequent polarization of atrial and ventricular heart muscles during each cycle, and this changes the electric potential near the heart. Because the tissues and blood of the body contain conductive ions, such changes in potential cause changes in currents and the net results affect the electric potential very far from the heart. As such, the cardiac muscle can be viewed as being placed in a volume conductor.

Why does this potential change with time, even for a single muscle cell? Let us follow the motion of charges during a cycle. The field across the cell membrane can be modeled locally as an electric dipole, with positive and negative charges, of equal magnitude, separated by a distance (Fig. 12.1). The electric field lines are shown for such a point dipole in Fig. 12.1.

A polarized cardiac muscle cell is a series of such dipoles as depicted in Fig. 12.29a, with about $-70\,\mathrm{mV}$ inside the cell relative to the outside, all around the cell. No potential (which is really a baseline potential) is seen at the electrode immediately to the right of the cell. As the depolarization wave propagates from left to right, the potential on the right increases and reaches a maximum when half the cell is depolarized, as in (c). As the depolarization wave arrives at the right end, this voltage decreases to zero as in (e). This is similar to the PQR wave in ventricular depolarization seen in the EKG in Fig. 12.28. This is what would occur if the potential across the membrane were zero after depolarization. Because it actually becomes slightly positive, the potential in (e) should dip slightly negative, as seen for the PQR wave. When the left side becomes repolarized, the potential becomes negative and a negative pulse develops, as in (f)–(h). This is similar to the S ventricular repolarization pulse in Fig. 12.28 except for its sign. Unlike that in Fig. 12.29h,

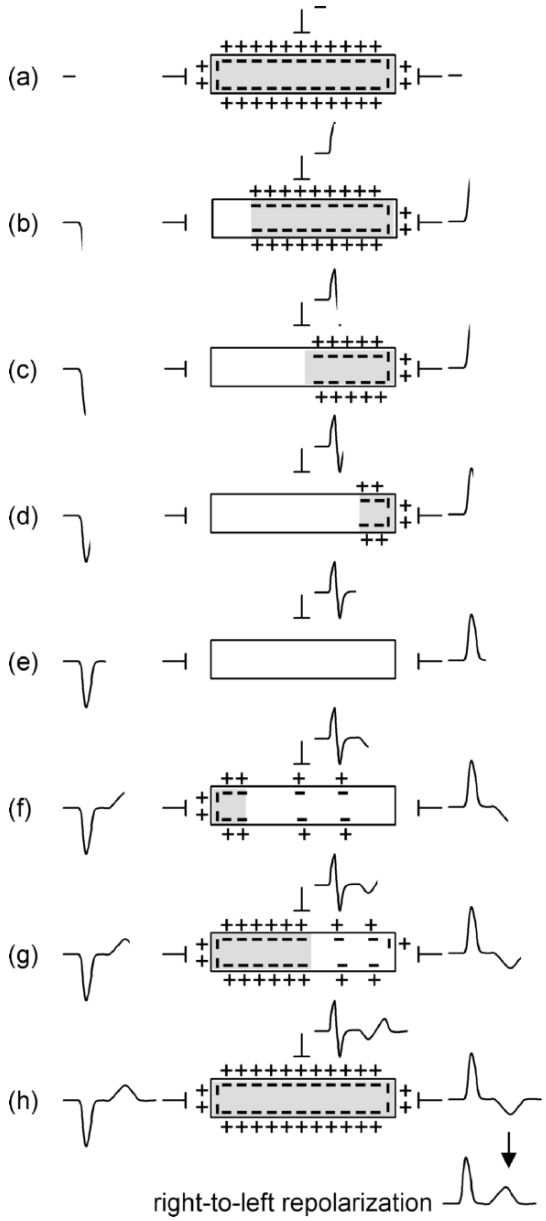

Fig. 12.29. Potential to the right of a strip of myocardium immersed in a volume conductor during (**a**)–(**e**) depolarization and (**f**)–(**h**) repolarization. The polarized section is gray and the depolarized section is white. For real cardiac muscle, the repolarization signal is positive, as is the depolarization signal (Fig. 12.28), because in the human heart repolarization proceeds in the direction opposite from depolarization, as shown on the bottom. (Based on [597])

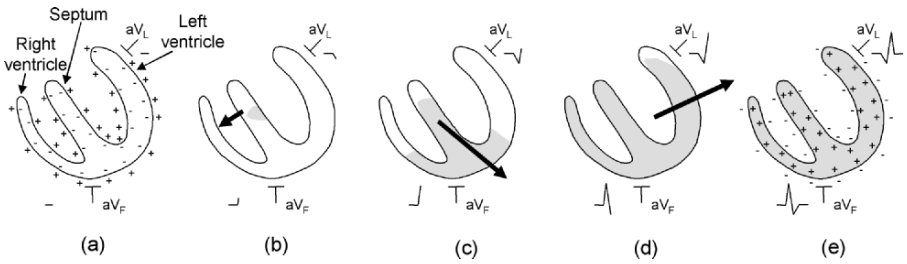

Fig. 12.30. Normal ventricular depolarization recorded by leads aV_L and aV_F, showing the change in magnitude and counterclockwise rotation of the projection of the cardiac dipole in the frontal plane. (Based on [584])

the second peak is positive because cardiac muscle repolarization proceeds in the direction opposite from depolarization, as for the lowermost trace. Furthermore, repolarization is a bit slower and more inhomogeneous than depolarization so the negative dip is broader (slower) and has a smaller magnitude (wider) than the first peak.

Figure 12.29 also shows that the potential is qualitatively different at the left and at the top of the cell during depolarization. This is why the EKG electrodes placed at different positions sense different signals (and can provide different information). Furthermore, the electrode placed on the left in Fig. 12.29 gives the negative of the signal of that placed on the right. (This makes sense. Why?)

Each of the four cycles of atrial and ventricular depolarization and atrial and ventricular repolarization does not occur simultaneously throughout the heart, and each is sensed by an EKG and can be analyzed separately. The evolution of the net cardiac electric dipole during ventricular depolarization (QRS cycle) is shown for a normal heart in Fig. 12.30.

Clearly the magnitude and direction of the dipole change greatly during each cycle. These are sensed by the exact placement of EKG electrodes, which can provide important details about cardiac function and malfunction. The location of the twelve leads for an EKG with a supine (lying down) person are described in Table 12.6. Six are on the ribs, and six others are on the arms and legs. Three of the latter have two leads (bipolar), one for monitoring and one for reference, while the other nine are single leads (unipolar). Figures 12.31 and 12.32 show the nine locations in the table where the 12 EKG leads are placed. Remember that voltage differences are being measured from one lead to another.

The earlier discussion shows that the EKG voltage is positive when the cardiac dipole points to the (positive side of the) EKG lead and negative when it points away from it. This is clear from Fig. 12.1d. Figure 12.33 shows the 12 EKG signals from a normal heart. Figure 12.30 shows the relation between the effective positioning of two of these bipolar leads, the evolution of the cardiac dipole, and the signal recorded by these leads.

Table 12.6. Position of electrodes in an EKG. See Figs. 12.31 and 12.32. (Using information from [575])

lead	electrode position
standard limb leads (bipolar)	
I	right arm and left arm
II	right arm and left leg
III	left arm and left leg
augmented leads (unipolar)	
aV_R	right arm
aV_L	left arm
aV_F	left leg
chest leads (unipolar)	
V_1	4th intercostal space, right side of sternum
V_2	4th intercostal space, left side of sternum
V_3	5th intercostal space, left side (between V_2 and V_4)
V_4	5th intercostal space, left side (midclavicular line)
V_5	5th intercostal space, left side (anterior axillary line)
V_6	5th intercostal space, left side (midaxillary line)

Three of the EKG electrodes are placed on the right and left arms and the left leg, and the voltages across the three pairs of these electrodes are monitored (along with the signals from the other probes), and are called I ($V_{\rm I} = V_{\text{left arm}} - V_{\text{right arm}}$), II ($V_{\rm II} = V_{\text{left leg}} - V_{\text{right arm}}$), and III

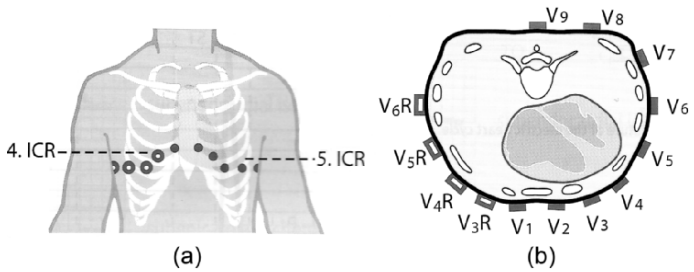

Fig. 12.31. Placement of the horizontal plane, precordial unipolar EKG electrodes. Only 6 of the 12 leads in (**b**), V_1–V_6, are used in usual EKGs (*solid circles*, in the region labeled by 5.ICR (5^{th} intercostal space or region in the ribs) in (**a**)). The additional dorsal leads V_7–V_9 are specifically used to detect a posterior myocardial infarction. The additional right precordial leads, V_3R–V_6R (*open circles*, in the region labeled by 4.ICR (4th intercostal space or region) in (a)), are specifically used to detect a right ventricular myocardial infarction. (From [577])

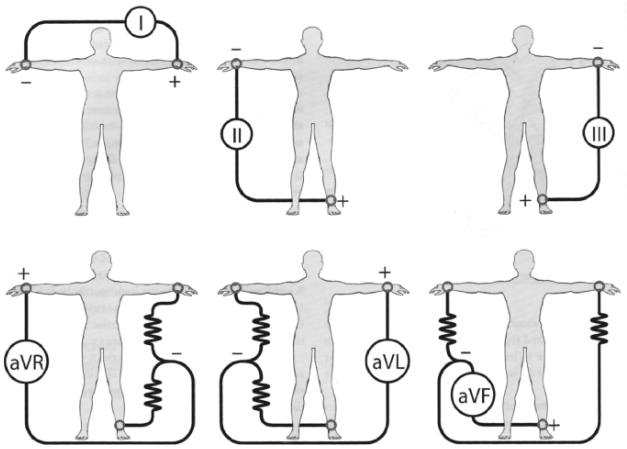

Fig. 12.32. Placement of the three unipolar and three bipolar front-plane limb leads. Sometimes an electrode is positioned on the right leg (not shown) to serve as an electrical ground. (From [577])

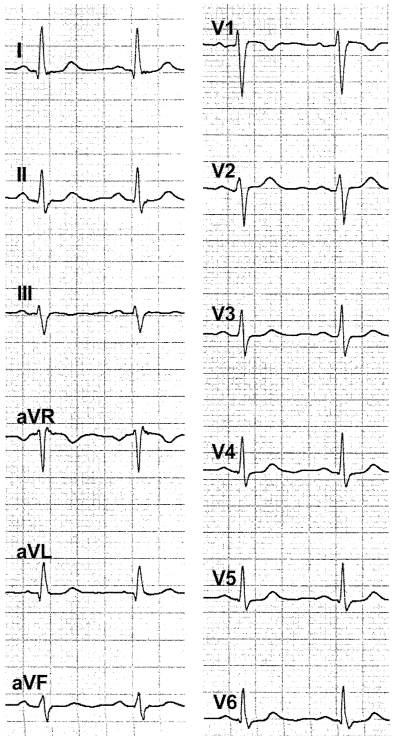

Fig. 12.33. Normal EKG patterns from the 12 electrodes. (From [577])

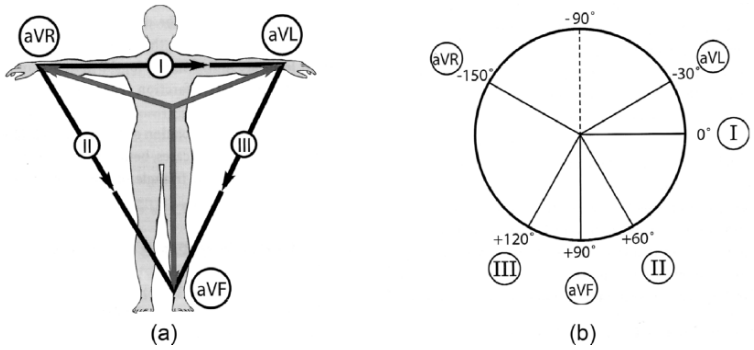

Fig. 12.34. (**a**) The three leads I, II, and III are arranged as Einhoven's triangle. (**b**) The effective directions for the six frontal leads shown in (a) are translated to form the triaxial reference system called Cabrera's circle. The signed, vector projection of the cardiac dipole onto these six directions gives the EKG signal for these six frontal plane leads. (From [577])

($V_{\rm III} = V_{\rm left\ leg} - V_{\rm left\ arm}$), as in Table 12.6. These three electrodes act as if they probe at the vertices of a triangle, which is usually called the *Einhoven's triangle*, as shown in Fig. 12.34a. Because the arms and legs do not have new sources of electric fields and the tissue in each is a conductor, the probes on the arms actually sense the same voltages as if they were instead placed on the respective shoulders and the probe on the leg has the same voltage as if it were placed on the bottom of the torso near the pubic area, and Einhoven's triangle is sometimes depicted for this smaller triangle. Using Kirchhoff's 2nd Law, (12.14), $V_{\rm I} + V_{\rm III} - V_{\rm II} = 0$ (the minus sign in front of the last potential indicates a different sign convention around the circuit than for the first two) or

$$V_{\rm I} + V_{\rm III} = V_{\rm II}. \tag{12.88}$$

Cabrera's circle in Fig. 12.34b shows the effective positioning of the six frontal plane leads, and this is used in Fig. 12.30.

Figure 12.34 shows how momentary cardiac dipoles in three-different directions cause momentary potential differences in these three electrode pairs. An appropriate sum of these three voltages, such as $V_{\rm I} + V_{\rm III} - V_{\rm II}$, serves as the electrical ground for measurements with each of the six chest probes. Also, note that the difference in the signals from the $\rm aV_L$ and $\rm aV_F$ leads in Fig. 12.30 should be similar to that from the III lead.

This EKG can provide important details about cardiac function and malfunction, and the location of the malfunction. This includes (1) the heart rate, (2) arrhythmia, (3) axis (giving the direction and magnitude of activity for atrial and ventricular contractions), (4) hypertrophy (which is an increase in the left or right ventricular muscle mass), (5) enlargement (which is an increase in the volume of the left or right atria chambers), and (6) infarction.

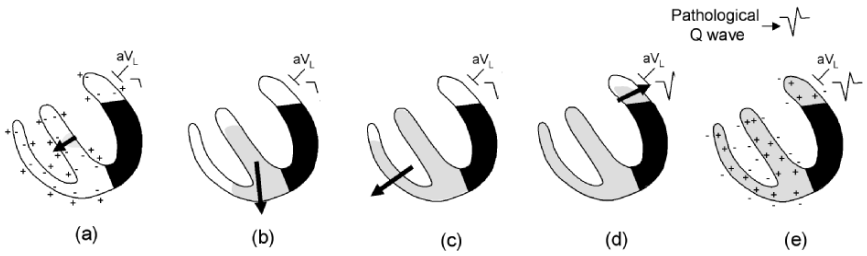

Fig. 12.35. Evolution of the cardiac dipole during ventricular depolarization after a lateral wall cardiac infarction, along with the EKG from lead aV_L. The larger-than-normal Q wave occurs because the site of the infarction (black) should be depolarizing and contributing a positive signal in (**c**). (Based on [584])

In arrhythmias, there can be a variable rhythm, a rhythm that is either too fast (tachycardia, >100 beats/min; but >250 beats/min – flutter or fibrillation – it can be life-threatening in the ventricles) or too slow (bradycardia, <60 beats per min, except it can be lower in trained athletes), and deviations from a 1:1 ratio of atrial and ventricular contractions, as described more in Chap. 8.

During a myocardial infarction part of the cardiac muscle is damaged and within a few hours these muscle cells usually die and then do not depolarize and repolarize. The absence of electrical signals from a given part of the left ventricle is seen in the EKG in Fig. 12.35. The dipole vector during depolarization points away from the black region of the infarction in step 3; if that black region were active it would then depolarize and the dipole would be pointing in the opposite direction. This is seen as an enhanced Q-wave. The formation of scarring in this damaged region can still be seen after recovery (Fig. 12.36).

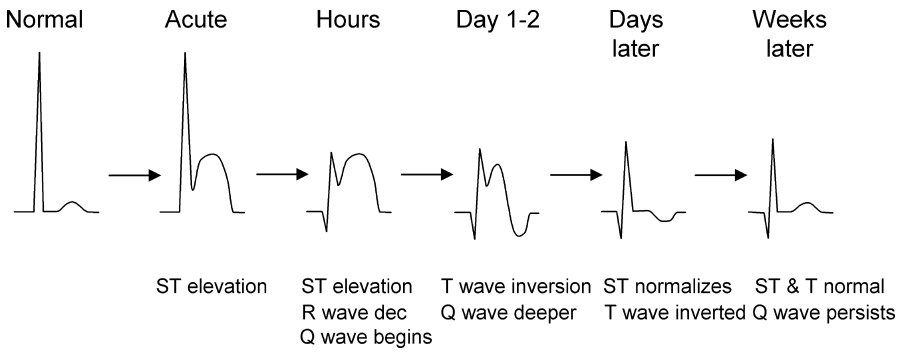

Fig. 12.36. EKG evolution during and after an acute Q-wave myocardial infarction. (Based on [584])

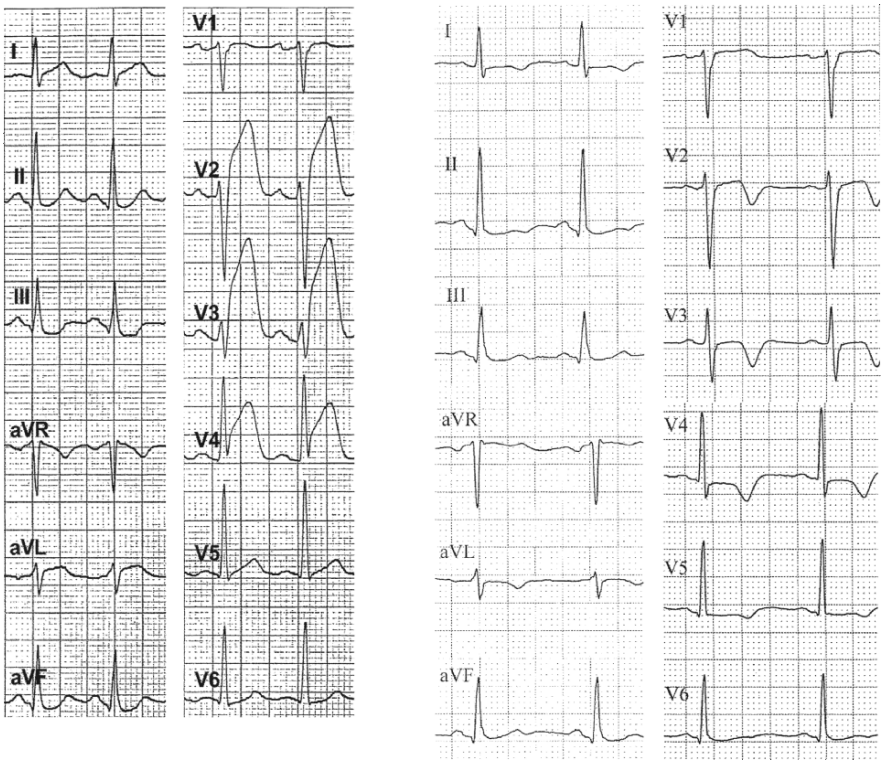

Fig. 12.37. EKG signals from the 12 leads (left) 2 h after an anteroseptal myocardial infarction an (right) 4 h later, after thrombolysis. (From [577])

In general, large Q waves in the I and aV_L traces indicate a lateral infarction, in the V_1, V_2, V_3, or V_4 traces an anterior infarction, and in the II, III, and aV_F traces an inferior infarction. A large R wave in the V_1 and V_2 traces indicates a posterior infarction.

Figure 12.37 shows all 12 EKG traces 2 h after an anteroseptal myocardial infarction (i.e., one with features of both anterior and (interventricular) septal myocardial infarctions) and 4 h after the infarction has been treated by thrombolysis (treatment to break up blood clots); there is no pathological Q wave in this case, but elevated ST waves at 2 h and a normal ST segment 4 h later, but negative T in some traces. (Compare both to the normal traces in Fig. 12.33.)

Information from these scalar measurements can be projected onto different body planes and provide information about the evolution of the cardiac dipole vectors in a process called vectorcardiography. Figure 12.38 shows the QRS vector evolution in a vectorcardiogram and its projections on the frontal and horizontal planes. For more on EKGs and diagnosis using EKGs see [572, 577, 584, 586, 587, 590, 591, 596, 597].

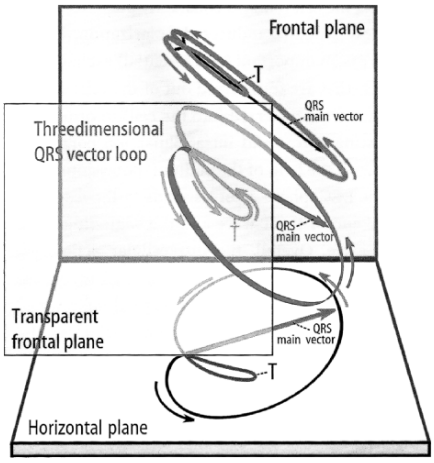

Fig. 12.38. A ventricular vectorcardiogram, showing the evolution of the QRS vector along its loop, along with its projections on the frontal and horizontal planes. The frontal projection gives the frontal plane EKG derived from the frontal plane leads, which need little correction; whereas the horizontal projection must be corrected to obtain the scalar EKG obtained directly from the precordial leads. (From [577])

12.6 Electrical Signals in the Brain

Electrical signals are also important in other parts of the body, as shown in Table 12.1, such as the electroencephalograms (EEGs) of brain waves in Fig. 12.39. In contrast to the very regular EKG patterns, the EEG signal is irregular, but it has identifiable rhythmic patterns: alpha waves (frequency of 8–13 Hz; awake, restful state), beta waves (14–25 Hz; alert wakefulness, extra

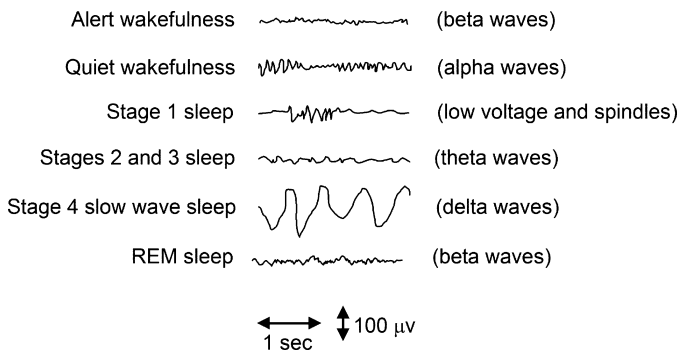

Fig. 12.39. Schematic of changes in brain waves during different stages of wakefulness and sleep. (Based on [580, 593])

Table 12.7. Effect of currents (in mA) on the human body (for about 1 s). (Using data from [595])

effect	DC	AC (60 Hz)
slight sensation at contact point	0.6	0.3
perception threshold	3.5	0.7
shock		
– not painful, no loss of muscular control	6	1.2
– painful, no loss of muscular control	41	6
– painful, let-go threshold	51	10.5
– painful, severe effects: muscular contractions, breathing difficulty	60	15
– possible ventricular fibrillation (loss of normal heart rhythm)	500	100

All values are approximate.

activation, tension), theta waves (4–7 Hz, mostly in children, also adults with emotional stress and with many brain disorders), and delta waves (<3.5 Hz; deep sleep) [586].

12.7 Effects of Electric Shock

External electrical currents running in the body can cause damage by interfering with normal bodily function – such as by preventing your otherwise operational skeletal and cardiac muscles from functioning normally – and by destroying tissues by thermal heating (Table 12.7). Muscles are controlled by a series of electrical impulses sent by the brain. External AC currents (60 Hz) above 10 mA or so override these signals and prevent you from exercising control over your muscles. You can barely control your muscles at 10 mA and barely "let go" of an object. At higher currents your muscles are under external control, possibly leading to breathing and circulatory difficulties. Ventricular fibrillation occurs from 100 mA to 4 A and paralysis occurs, along with severe burns (and death), over 4 A. For weak shocks, the sensation of shock varies as the 3.5 power of the applied 60 Hz voltage (Stevens' Law (1.6), Table 1.15), so the perception of electric shock is very superlinear with stimulus.

The skin is a very important barrier to current flow (I). The resistance (R) through dry skin is roughly 100,000–600,000 ohms and through wet skin it is only about 1,000 ohms. If the skin barrier is overcome, the resistance drops (so there is more current flow per unit voltage, as per Ohm's Law). Figure 12.40 shows that the internal body resistance is low, approximately 400–600 ohms from head to foot and 100 ohms from ear to ear. The amount of current that can flow in the body induced by a voltage source (V) is limited by two factors

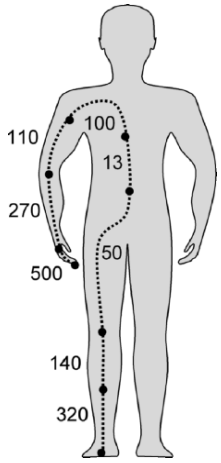

Fig. 12.40. Body segment resistance (in ohms), ignoring skin contribution. As shown, 500 ohms is the contribution from one finger. (Based on [579])

(1) Ohm's Law says the current will be $I = V/R$. (2) The current is sometimes limited by the voltage source itself.

Let us assume the skin barrier has been broken so the effective body resistance is about 500 ohms. (Please do not attempt this!!!) The 120 V AC from a wall outlet will produce a current of 240 mA, which is over twice that needed to cause death through ventricular fibrillation. Circuit breakers typically trip at 15 A, so this flow through the body will be uninterrupted by the circuit breaker. How about DC sources? The current induced by the often-used 9 V battery is 18 mA, which can cause a shock. (You can easily draw this current from such a battery.) The voltage across a car battery is 12 V with 400–600 A (cranking amps), so it can shock you even worse (Problem 12.5).

12.8 Magnetic Properties

The magnetic fields in the body are due to electric currents and are extremely weak. Typical magnetic fields in the body that can be measured are shown in Table 12.8, and are all much weaker than the 5×10^{-5} T (0.5 Gauss) magnetic field of the earth. (For comparison, the maximum human-made magnetic fields approach 100 T.)

12.8.1 Magnetic Field from an Axon

The Biot-Savart Law determines the magnetic field from currents. Consider a continuous current I flowing along the infinitely long z-axis. Using the Biot-Savart Law, one can show that a distance R away the magnetic field B has a

Table 12.8. Typical amplitude of biomagnetic signals. (Using data from [567])

biomagnetic signal	typical amplitude (pT)
magnetocardiogram (MCG)	50
fetal MCG	1–10
magnetoencephalogram	1
evoked fields	0.1
magnetomyogram	10
magneto-oculogram	10
Earth's field	50×10^6

magnitude

$$B = \frac{\mu_0 I}{2\pi R} \tag{12.89}$$

and is in the radial direction, according to the usual right hand rule.

This analysis does not exactly apply to signals along a neural axon. A voltage pulse traveling along an axon is a pulse and not a continuous current. It is in a medium that is fairly conductive. Also, there are several directions of the current flow, along the axon, transverse to the membrane, etc. Still, let us estimate the field strength just as the pulse passes by, and model it as a continuous current. The current along the axon is the most important. Using (12.63) $I_{\rm i}(x) = -(1/r_{\rm i}){\rm d}V/{\rm d}x$, we estimate the magnitude of this current to be

$$I \sim \frac{1}{r_{\rm i}} \frac{V}{\lambda}. \tag{12.90}$$

Therefore, the magnetic field magnitude 1 mm away from the axon is approximately

$$B \sim \frac{\mu_0 V}{2\pi R r_{\rm i} \lambda} \tag{12.91}$$

$$= \frac{(4\pi \times 10^{-7}\ \text{T-m/A})(0.1\ \text{V})}{2\pi(0.001\ \text{m})(6.4 \times 10^9\ \text{ohm/m})(3.8 \times 10^{-4}\ \text{m})} = 8\ \text{pT}, \tag{12.92}$$

with $\lambda = 3.8 \times 10^{-4}$ m. This value is consistent with the low values in Table 12.8. (This estimate is reasonable even though some of the assumptions are not perfect.)

12.8.2 Magnetic Sense

Humans (apparently) cannot sense magnetic fields, but magnetic fields do help several animals sense direction (as with a compass) and/or location due to the presence of 50-nm diameter magnetite (Fe_3O_4) particles in their bodies. (These particles are sometimes arranged in chains.) For example, this

magnetic sense is very strong in pigeons, who have 10–20 nT sensitivity, and dolphins, who have $<2\,\mu$T sensitivity [565]. The magnetic sense mechanism may involve a torque that is induced on this particle system by the field and this in turn may induce a torque on intracellular filaments; this movement of the filaments triggers a sensory neuron. (Electric fields induce a torque on an electric dipole, as is easily seen by examining the Coulomb forces on the individual charges in the electric dipole. Similarly, magnetic fields induce a torque on a magnetic moment. This analogy is valid even though there are no magnetic charges.)

12.9 Electromagnetic Waves

Radio waves, microwaves, infrared radiation, visible light, ultraviolet light, X-rays, and gamma rays are all electromagnetic waves. Each propagates at the same speed of light c in vacuum. Each has a frequency of oscillation ν and wavelength λ related by $c = \lambda\nu$ (11.2). For each, this oscillation consists of electric and magnetic fields sinusoidally oscillating in phase in vacuum. They differ only in their frequency (and consequently wavelength), which increases (decreases) in going from one of these regimes to the next. We discussed visible light at length in Chap. 11.

The penetration of electromagnetic radiation through the body is sometimes of interest. The attenuation factor for such radiation plotted in Fig. 12.41 is α_{light} from Beer's Law, (10.18),

$$I(z) = I(z = 0) \exp(-\alpha_{\text{light}} z). \tag{12.93}$$

Attenuation consists of losses from absorption and scattering, and is clearly very dependent on frequency. This figure shows trends, but not all details. For example, the attenuation factor in the microwave is due to nonresonant processes. The body absorbs microwave radiation at 2.45 GHz used in microwave ovens much more strongly than indicated there because of the strong resonant absorption by water at this frequency. (This is why this frequency is used in microwave ovens.)

12.10 Summary

Electrical processes are essential to the operation of the body and have proved to be very important in medical diagnostics. Electrical conduction is important in most parts of the body. Models of the propagation of electrical signals in nerves can explain the physical basis of perhaps the most important mechanism of regulation in the body. Electrical processes are integral to cell operation, including to the physics of cell membranes. The electrical nature of the heart has led to the use of EKGs as a diagnostic that can be interpreted

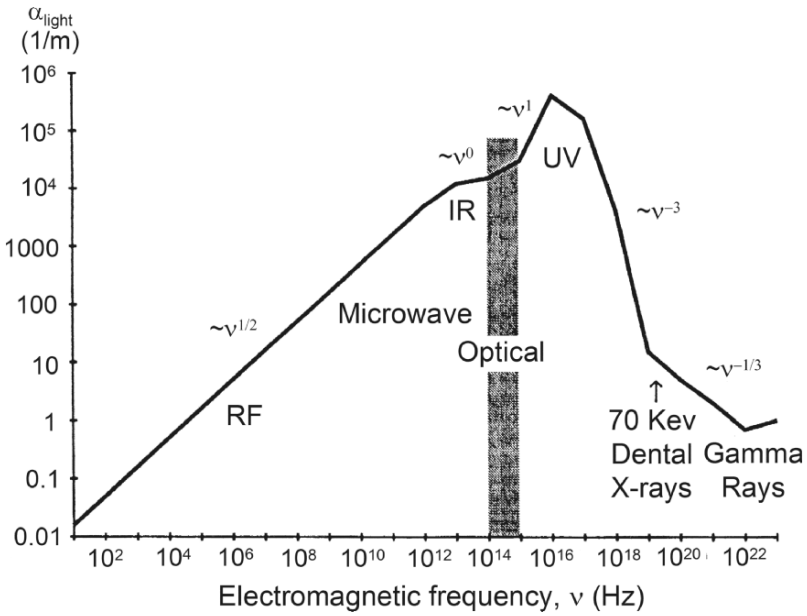

Fig. 12.41. Attenuation of electromagnetic radiation in human tissue, due to absorption and scattering. (From [576]. Courtesy of Robert A. Freitas Jr., Nanomedicine, Vol. 1 (1999), http://www.nanomedicine.com)

by using simple models of the dipole nature of the heart. Electrical signals in other parts of the body are also used in diagnostics. Naturally occurring magnetic signals are relatively less important in the body.

Problems

Conductance, Transmission, and Potentials

12.1. Use Table 12.4 to compare the conductivity in a cell and in blood.

12.2. Estimate the electrical resistance of the blood in a 50-cm long, 3-mm diameter artery.

12.3. There are two common relations for the resistivity of blood as a function of the hematocrit Hct: $\rho = 0.537\exp(0.025\text{Hct})$ and $\rho = 0.586(1 + 0.0125\text{Hct})/(1 - 0.01\text{Hct})$, which is called the Maxwell–Fricke equation [586]. How do they differ in the range of Hct from 10%–60%, and specifically at the normal value of 45%?

12.4. During an accident, 120 V AC from a wall socket connects your body to electrical ground, from hand to hand:

(a) If the resistance across the body is 500 ohms, what is the current flow?
(b) Is this dangerous?
(c) If the region from hand to hand can be modeled as a cylinder of constant diameter (equal to the diameter of the upper arm) and length (from finger tip to finger tip) of your own body, and all material is assumed to be uniform, estimate the electrical resistivity of the body tissue.
(d) How much power is dissipated in this section? (Calculate both the total power and the power per unit volume.) (Remember that the power dissipated is $P = IV$ and Ohm's Law is $V = IR$. Assume here and below that the power is the same as that for a DC voltage source.)
(d) What is the heat capacity of this cylindrical section? Assume the average specific heat of the body.
(e) Ignoring heat flow, how much would the temperature of this section increase per unit time?
(f) How long would it take to denature the proteins in this cylindrical section? (See the information provided in Chap. 13.)

12.5. Compare the amount of current that could be drawn from a car battery in an electrical shock to the maximum amount of current that could be drawn from it. What does this mean? Why is the shock worse than that from a 9-V battery?

12.6. What ranges of electromagnetic radiation can penetrate through your (a) eyelid, (b) finger, and (c) chest?

12.7. An ion of mass m and charge q moves at a speed v under the influence of an electric field E. It suffers a drag force that relaxes its speed with a characteristic time τ:
(a) Show that force balance on the charge gives: $m\mathrm{d}v/\mathrm{d}t = -mv/\tau + qE$.
(b) Show that in steady state, the ion moves at the drift velocity (which is really the drift speed here), $v_{\mathrm{drift}} = qE\tau/m = \mu E$, where $\mu = q\tau/m$ is called the mobility.

12.8. (advanced problem) Show that the potential of a charge Ze shielded by mobile charges is given by $V(r) = (Ze/4\pi\epsilon_0\epsilon r)\exp(-\kappa r)$, where $\kappa = \sqrt{(e^2/\epsilon_0\epsilon k_{\mathrm{B}}T)\sum_i Z_i^2 n_{i,0}}$. Do this by substituting this solution for $V(r)$ into the Poisson–Boltzmann equation (12.41), which can be expressed in three-dimensions as:

$$\frac{1}{r}\frac{\mathrm{d}^2(rV)}{\mathrm{d}r^2} = -\frac{1}{\epsilon_0\epsilon}\sum_i Z_i e n_{i,0}\exp(-Z_i eV/k_{\mathrm{B}}T) \tag{12.94}$$

for this spherically symmetric potential. Assume the region is electrically neutral and that $Z_i eV/k_{\mathrm{B}}T \ll 1$. (Hint: See Appendix C.)

12.9. (advanced problem) Repeat Problem (12.8), this time solving the Poisson–Boltzmann equation under the stated conditions in one-dimension. How does this solution differ from the spherically-symmetric three-dimensional solution?

12.10. In her famous 1973 rendition of the song "Killing Me Softly With His Song," Roberta Flack sang, "He sang as if he knew me in all my dark despair. And then he looked right through me as if I wasn't there." [578] If this were literally true, electromagnetic radiation would have to be able to be transmitted through her body. Over what wavelength ranges would that be possible? (Of course, there would also have to be a source of such radiation and his eyes would have to be sensitive to those wavelengths.) (By the way, this song was written by Norman Gimbel and Charles Fox for Lori Lieberman, who sang it in 1971, and it was sung in the 2001 movie, "About a Boy." A modified version was also released by the Fugees in 1996, however without the cited lyrics.)

Neuron Transmission and Membranes

12.11. Which of the four mechanisms involved in ion transport in an axon membrane shown in Fig. 12.11 contribute to the negative charge inside the cell and which to the positive charge?

12.12. The capacitance of a cylinder of length L, inner radius a, and outer radius $a + b$, with electrodes separated by material with dielectric constant κ, is $C_{\text{cylinder}} = 2\pi\kappa\epsilon_0 L/\ln(1+b/a)$. Show that unfolding the cylinder and treating it as a parallel plate capacitor is an excellent approximation for unmyelinated axons, but not for myelinated axons.

12.13. (a) Estimate the effective dielectric constant κ of myelin, by suitably weighting the averages of the dielectric constants of its components. These water, lipid, and polar components have $\kappa = 80$, 2.2, and 50, respectively, and have effective thicknesses t of 2.2, 4.2, and 10.8 nm, respectively, in the repeated 17.1 nm bilipid layered structure in the myelin [581]. These can be considered as capacitances in series, so

$$\kappa_{\text{eff}} = \frac{t_{\text{total}}}{t_{\text{water}}/\kappa_{\text{water}} + t_{\text{lipid}}/\kappa_{\text{lipid}} + t_{\text{polar}}/\kappa_{\text{polar}}}. \tag{12.95}$$

(b) How does this answer help explain why $\kappa = 7$ is reasonable for the axon membrane?

12.14. (advanced problem) Derive the relation in Problem 12.13(a).

12.15. Compare the numerical values of the graded potential decay length λ for typical unmyelinated and myelinated axons.

12.16. It is assumed that the spatial decay of the graded potential in myelinated axons is slow enough that there is little decay before the signal reaches the next node of Ranvier for regeneration. Is this assumption valid?

12.17. Some pain receptors transmit signals on myelinated axons in neurons with conduction speeds up to 30 m/s and others are transmitted on very slow unmyelinated axons with speeds of 2 m/s and lower. How long does it take such receptors on your finger tips to be transmitted to your brain?

12.18. Show that the conduction speeds as given in the caption of Fig. 12.22 are consistent with the EMGs given in the figure.

12.19. Determine the characteristic time τ for unmyelinated and myelinated axons.

12.20. Use substitution to show that (12.80) is the solution to (12.79).

12.21. Use substitution to show that (12.83) is the solution to (12.82).

12.22. Show that substituting (12.84) into (12.72) gives (12.85).

12.23. (advanced problem) Use substitution to show that each of the following is a solution to the voltage along an axon cable in steady state (12.79) for $V_i = 0$:

$$V(x) = A_1 \exp(x/\lambda) + A_2 \exp(-x/\lambda), \tag{12.96}$$

$$V(x) = B_1 \cosh(x/\lambda) + B_2 \sinh(x/\lambda), \tag{12.97}$$

$$V(x) = C_1 \cosh((x-L)/\lambda) + C_2 \sinh((x-L)/\lambda). \tag{12.98}$$

12.24. (advanced problem) Use substitution and evaluation at the boundaries to show that each of the following is a solution to the voltage along an axon cable (for $x \geq 0$) in steady state (12.79) as in Fig. 12.24, for $V_i = 0$ as the boundary condition $V(x = 0) = V_0$ and [589]:
(a) An semi-infinitely long cable (Fig. 12.24a):

$$V(x) = V_0 \exp(-x/\lambda), \tag{12.99}$$

(b) A cable of length L and the boundary condition that $V = 0$ at $x = L$ (which means the voltage is clamped at zero at the end of the cable, which is a *short-circuit boundary condition*) (Fig. 12.24b2):

$$V(x) = V_0 \, \frac{\sinh((L-x)/\lambda)}{\sinh(L/\lambda)}. \tag{12.100}$$

(c) A cable of length L and the boundary condition that $\mathrm{d}V/\mathrm{d}x = 0$ at $x = L$ (which means zero core current at the end of the cable, which is an *open-circuit boundary condition*) (Fig. 12.24c2):

$$V(x) = V_0 \, \frac{\cosh((L-x)/\lambda)}{\cosh(L/\lambda)}. \tag{12.101}$$

(d) A cable of length L and the boundary condition that $V = V_\mathrm{L}$ at $x = L$ (which means the voltage is clamped at $V = V_\mathrm{L}$ at the end of the cable)

(Fig. 12.24d):

$$V(x) = \frac{V_0 \sinh((L-x)/\lambda) + V_\mathrm{L} \sinh(x/\lambda)}{\sinh(L/\lambda)}. \tag{12.102}$$

12.25. Sketch V in (12.83) vs. t. (Label $t = \tau$.)

12.26. Sketch V in (12.87) vs. t and also vs. x. (Label $t = \tau$ and $x = \sqrt{D_\mathrm{diff} t}$, in the respective sketches.)

EKGs

12.27. By a series of diagrams similar to Fig. 12.29, show that the repolarization waves traveling to the left and right, respectively, produce signals that are the negative of each other.

12.28. Find the heart rate from the EKGs in Fig. 12.33. Each big box is 0.2 s wide.

12.29. Show that the integration of the cardiac dipole electric field gives a potential that is positive at a point the dipole points to, negative at a point the dipole points away from, and zero at a point where the dipole points in a transverse direction.

12.30. Assume that in (A)–(D) in Fig. 12.42 the cardiac dipole is initially zero, increases to the maximum dipole vector shown, and then decreases to zero, always in the direction shown. (This is not what normally happens. Why?) Match each dipole in (A)–(D) to the EKGs (a)–(d) for the EKG Type I lead shown.

12.31. Assume the same dipole dependencies as in Problem 12.30. Sketch the EKGs for EKG leads II and III for cases (A)–(D) in Fig. 12.42.

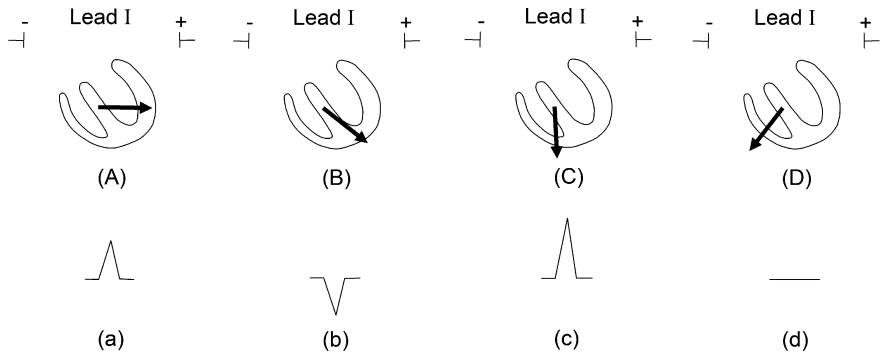

Fig. 12.42. Examples of cardiac dipoles and EKG lead I. (Based on [584].) For Problems 12.30–12.32

12.32. Explain why the sequence of cardiac dipole evolution is normally (D), (C), (B), (A) for the dipoles shown in Fig. 12.42.

12.33. (a) Use the normal sequence of cardiac dipole evolution to sketch the evolution of the EKG signal for EKG leads I, II, and III.
(b) The three lead potentials should always sum to zero. Confirm that your EKGs do so.

12.34. Compare the EKGs in Fig. 12.37 – taken at two times after a heart attack – with each other and then with the normal traces in Fig. 12.33.